University of Naples "Federico II"

Telethon Institute of Genetics and Medicine (TIGEM)

RESEARCH DOCTORATE (PhD) in

COMPUTATIONAL BIOLOGY and BIOINFORMATICS

"Reconstitution of an ultradian oscillator in mammalian cells by a synthetic biology approach"

Supervisor: Candidate:
Prof. Diego di Bernardo   Marco Santorelli

Coordinator:
Prof. Sergio Cocozza

ACADEMIC YEAR 2013/2016

«Quand'anche le vostre speranze fossero state deluse non sette volte,
ma settanta volte sette,
non rinnegate mai la speranza...
Quando un tentativo s'è fatto e non è riuscito,
bisogna guardarsi attorno,
e guardarsi dentro,
e riflettere attentamente,
e scoprire,
e confessarsi gli errori commessi,
e veder d'onde vengono,
e cercar le vie che potrebbero ripararli,
poi ricominciare da capo,
e una terza volta,
e una quarta,
e finché si riesca.
La nostra è guerra,
guerra mortale
guerra che si combatte secretamente da anni, da secoli,
e volete vincere alla prima battaglia...»

Giuseppe Mazzini

Contents

Chapter 1 - Introduction to synthetic oscillators

1.1 - Synthetic biological oscillators

Synthetic Biology can be defined as the engineering of biology. The core aim of this discipline is to develop and apply engineering approaches, to build new synthetic pathways (or circuits as they are referred to in this discipline). Using well characterized biological 'parts' this discipline focus to engineer new functions in the cell for biotechnological or medical applications[1].

Moreover, Synthetic biology aims to uncover the design principles of natural biological systems through the design of very simple synthetic circuit.[2]

For example, synthetic gene circuits that emulate the expression dynamics of living systems provide new insights into the connectivity of genes and they advance our understanding of complex networks.[3] In particular, in the last decades, much attention has been directed on the comprehension of the genetic oscillators, since in nature they underlie several biological processes[4,5].

A genetic oscillator is defined as a gene or a set of genes that working together are cyclically expressed in time. Several designs have been proposed for oscillator and they were implemented both in prokaryotic and mammalian cells.

Indeed, based on their network topologies they can be grouped in four different classes of oscillators: Goodwin oscillator[6,7,8], repressilators[9,10], amplified negative feedback oscillator[3,4,11] and Smolen oscillator[7,12] (Fig. 1.1). The first one, Goodwin oscillator, is the simplest genetic oscillator constituted by a single gene that repress its own expression (Fig. 1.1 a). This very simple network was implemented both in *E. coli* and in 3T3 mouse fibroblast cell line (Silver oscillator)[7,8].

The repressilator can be thought of as an extension of the Goodwin oscillator, that can be also considered a one-gene repressilator. This class of oscillator can be composed of one or more genes, each repressing its successor in the network[9,10] (Fig. 1.1 b).
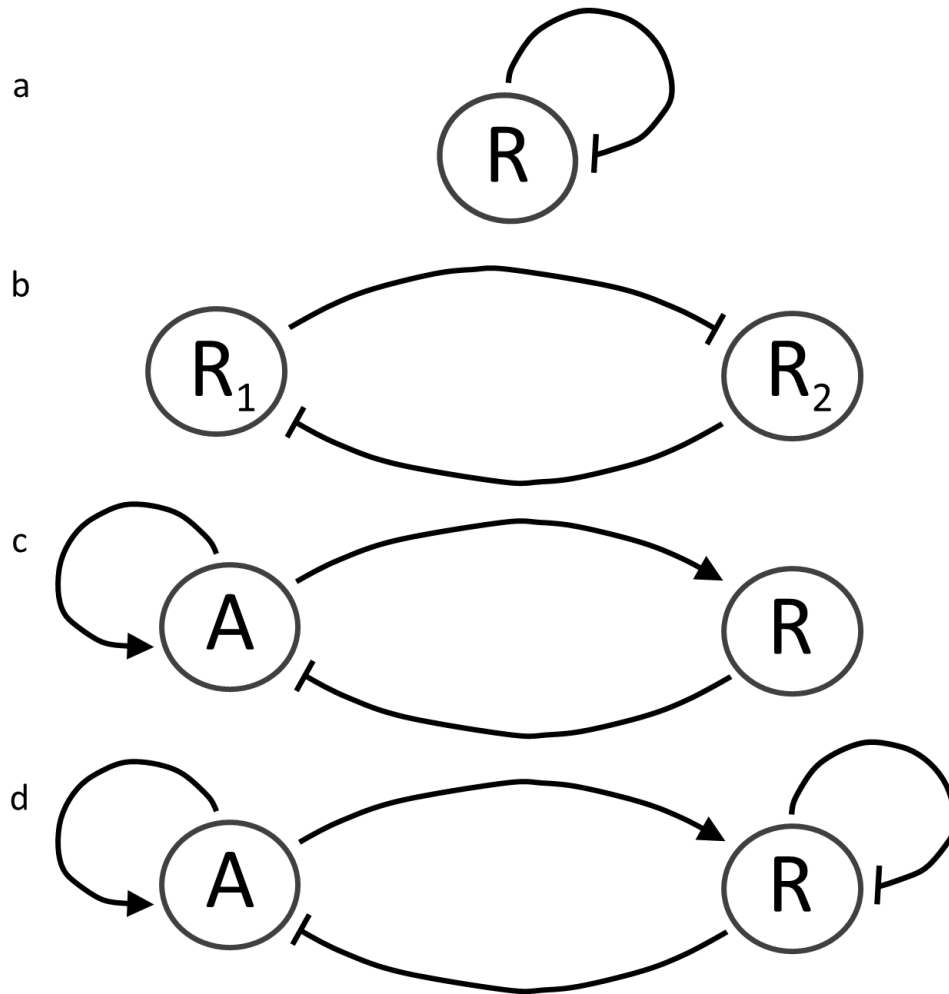
Figure 1.1 – Network topology of the different classes of the genetic oscillators. The circles marked with letter A are the activator whereas circles marked with letter R are the repressor. The arrows are the activating links whereas the other kind of links denoted repression activity. **(a)** The Goodwin oscillator, a mono-gene repressilator. **(b)** The repressilator. **(c)** The amplified negative feedback oscillator. **(d)** The Smolen oscillator.

In contrast to repressilators that are uniquely formed by repressive links, the amplified negative feedback oscillator also incorporates positive feedback (Fig. 1.1 c). Therefore, one gene promotes its own transcription via a positive self-feedback loop and also activates transcription of the other gene. At the same time, the second gene represses transcription of the first one, forming a negative feedback loop[4]. This topology has been implemented by transient transfection in mammalian cells by Fussenegger group[3,11].

Lastly, the Smolen oscillators[12] is constituted of two genes, and it differs from the amplified negative feedback oscillators for an auto-inhibition loop acting on the repressor gene. In particular, the first gene promotes its own transcription and that of the other gene, while the second gene represses its own transcription and that of the first gene[7] (Fig. 1.1 d).

In this chapter I will address my dissertation on Goodwin and Smolen oscillators, because they are the network topologies that I designed and implemented in this thesis work.

1.2 – The Goodwin oscillator

The Goodwin oscillator was the first and the simplest oscillator reported in literature. The circuit is composed by a single gene whose gene product represses itself expression[6](Fig. 1.2).
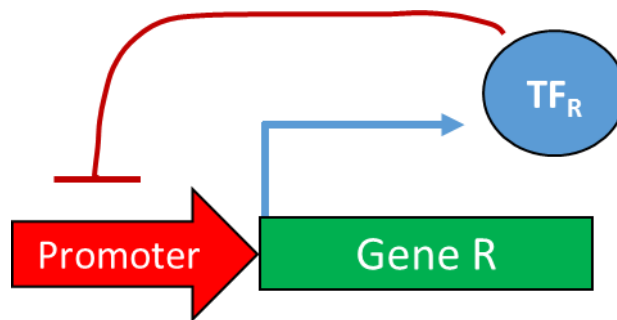
Figure 1.2 – Schematic representation of the Goodwin oscillator topology. The gene R product (TF$_R$) represses its own transcription by binding its own promoter.

This kind of oscillator has been described by a plethora of mathematical models based on ordinary differential equations (ODEs), delay differential equations (DDEs)[4,10]. These models have suggested that in the Goodwin network, oscillations can occur if repression is modelled by a nonlinear Hill function with a sufficiently high cooperativity coefficient[13,4].

Moreover, the presence of a time delay in the negative feedback loop has a constructive role, by expanding the parameters region where oscillations can happen. Nevertheless, the models suggested for this simple network only damped oscillations under biologically realistic parameters[7].

However, using stochastic simulations with parameters drawn randomly has been obtained sustained oscillations only under certain conditions, suggesting a parameter dependent constructive role of noise[4]. This particular topology of oscillator was implemented both in prokaryotes and mammalian cells. Experimental data show that the percentage of

oscillating cells is low showing relatively irregular oscillations, both in period and amplitude, often failing to return to a zero level.

1.3 – Mammalian implementation of the Goodwin oscillator: Silver oscillator

As previously described, synthetic biology by building simplified synthetic circuits aims to discovery the design principles and structure-function relationship that nature created in millions of years of evolution.

In humans, intron lengths contribute 95% of the average gene's sequence[14,8], one potential role is that they may work as modular time delays. In fact, their absence in developmentally expressed genes could alter the accuracy of timing and dynamics of developmental events[15,16,17,8].

In Pamela Silver Lab in 2008 was published a paper describing how the intron length can increase the time required to transcribe a gene, in order to understand the potential impact of introns on transcriptional time delay[8].

To this aim a set of three delayed Goodwin oscillators carrying three introns, of three different lengths, were produced. In particular, a negative feedback loop was engineered; in this circuit, the strong β-actin promoter drives the expression of a humanized Tet repressor (TetR) fused to the fast folded Venus variant of yellow fluorescent protein (YFP) (Fig. 1.3).
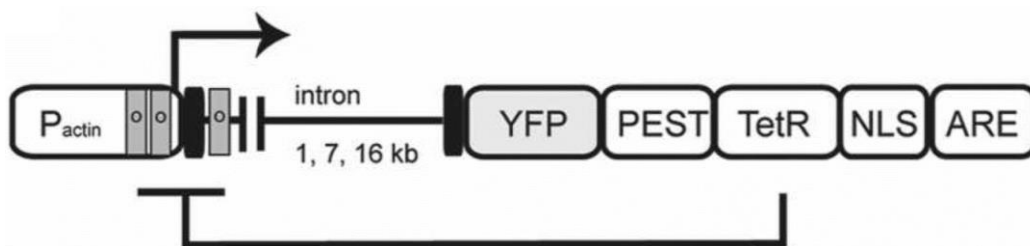
Figure 1.3 – **Schematic representation of Silver oscillators.** The engineered negative feedback is based on a humanized Tet repressor (TetR) that binds the modified promoter of the b-actin (P_{actin}) carrying several repetitions of the tet Operetor sequence (gray rectangle marked by the symbol o). The three reported circuit carryng three introns of three different length respectively (1 , 7 , 16 kb) Adapted from Swinburne et al. 2008.

The TetR fusion contains a nuclear localization signal (NLS) from SV40 necessary for the import of the protein to the nucleus, where it inhibits transcription initiation of its own gene by binding tet- operators (tetO) in the promoter region; a PEST sequence to the repressor protein and AU-rich elements (ARE) to the messenger were also added to reduce stability both at the protein and at mRNA level[8].

Repression can be removed by the addition of doxycycline. In this work they varied the size of the introns in the reporter gene by introducing intron of different lengths (1 kb, 7 kb or 16 kb). Clonal populations of 3T3 mouse fibroblast cell lines containing each of the three length variants of the negative feedback loop were generated[8].

From single cell data indicated that the pulse length distribution increase with gene length. The cause of this increase could be due to either transcription elongation alone or to the combined influence of transcription times and altered splicing rates[8].

The results suggest that intron length can indeed affect the dynamics of oscillatory expression; resulting effects, as has been proved[15], may be important in many contexts, such as in neural development during embryogenesis.

1.4 – The Smolen oscillator

Since oscillators are key component of cellular systems and they underlie complex decision in living cells, their robustness is vital.[18] However, from mathematical simulations and experimental data has been shown that the Goodwin oscillator is not very robust[4]. Moreover, in last decades more complex gene networks have been studied by a synthetic approach, in order to build a robust synthetic oscillator and thus studying the structure-function relationship. One example of complex circuit is the Smolen oscillator represented in Figure 1.4.

This network is composed of two genes, A and R. The gene product of the first gene (gene A) is the transcriptional activator (TF_A) and promotes its own transcription and that of the second gene (gene R) that express the transcriptional repressor (TF_R) and inhibits its own transcription and that of the gene A[12].

From a mathematical point of view, it was shown that oscillations are more likely to
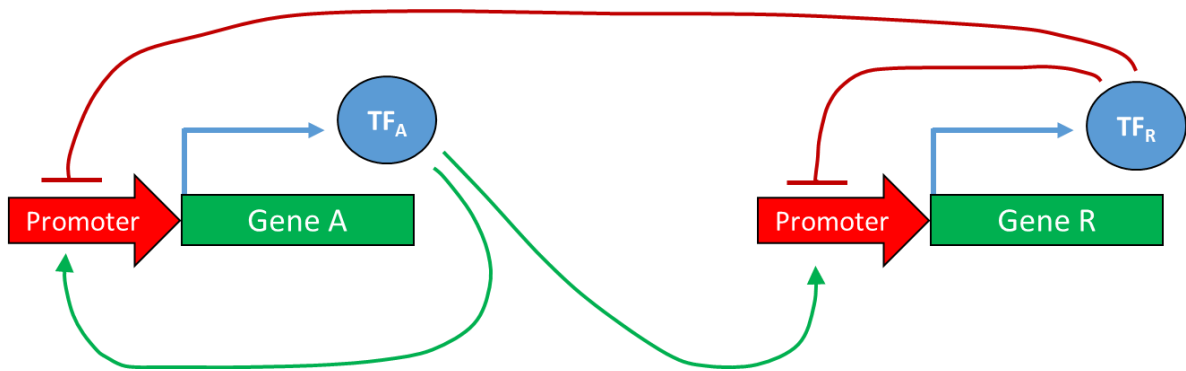
Figure 1.4 - Smolen oscillator topology. Gene A express a transcriptional activator that acts on its own promoter and on that of gene R, while gene R product (TF$_R$) represses its own transcription and that of gene A.

occur when the activator degradation rate is two or three times faster than that of the repressor. the role of the delay in oscillations was investigated for Smolen oscillator, however ambiguous results were obtained; therefore, the effects of delay on the dynamics of transcription regulation need to be clarified[4].

This network topology was implemented in *E. coli* and the results reveal that this oscillator is robust, fast and highly tunable[7]

1.5 – Prokaryotic implementation of the Smolen Oscillator

The synthetic gene oscillator presented in this section is based on the network topology of the Smolen oscillator and was implemented using *E. coli* components and hybrids synthetic promoters (Fig. 1.5).

The hybrid promoter, named plac/ara-1, is composed of the activation operator site from the araBAD promoter placed in its normal location relative to the transcription start site, and repression operator sites from the lacZYA promoter placed both upstream and immediately downstream of the transcription start site. It is activated by the AraC protein in the presence of arabinose and repressed by the LacI protein in the absence of isopropyl b-D-1-thiogalactopyranoside (IPTG). The araC, lacI and yemGFP (monomeric yeast-enhanced green fluorescent protein) genes were placed under the control of three identical copies of the hybrid promoter to form three co-regulated transcription modules. The modules expressing for the

yemGFP has no function in the oscillator, however it is used as a fluorescent gene reporter of gene expression[7].
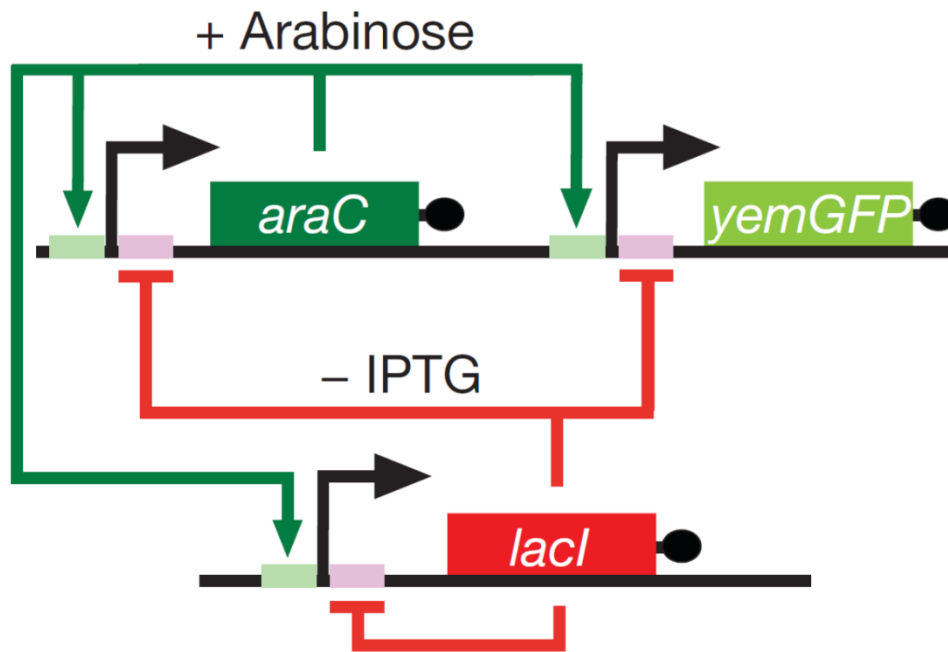
Using a time lapse fluorescent microscope for single-cell analysis interfaced with microfluidic platform, that precisely control environmental conditions, they demonstrated in this system almost every cell exhibited large amplitude oscillations. Moreover the Smolen network give rise to a tunable oscillatory periods ranging from 13 minutes up to 58 minutes[7]. These results are encouraging for possible use of this gene network in biotechnological applications and suggest a future implementation in mammalian cells. Moreover, the study of the network described in this section shed light on possible network topology underlie natural oscillator, because its rapidity, robustness and modulability are all characteristics observed in natural oscillators[4].

Chapter 2 - *Hes1*: an ultradian mammalian oscillator

2.1 – Introduction

Development is a highly organized process that depends on the timely proliferation of stem cells and their differentiation into multiple cell types. The balance between cell proliferation and cell fate determination is critical to forming organs with the right shape and size and the right cell composition[19].

Mammalian Hes factors play a central role in the development of many organs[20], working as effectors of the Notch signaling pathway, which coordinates cell proliferation and differentiation via cell-cell interaction[21]. In fact, in this developmental processes Hes factors maintain the progenitor cells in an undifferentiated state expanding in this way the pool of the progenitor cells[22,23].

Conversely, these genes regulate the binary cell fate decisions in many organs. In particular, has been demonstrated that some Hes factors, such as *Hes1*, are periodically expressed by a mechanism of auto-inhibition based on a negative feedback loop[24], these oscillations are fundamental for the maintenance of a pool of undifferentiated cell during the development of central nervous system. Indeed, has been demonstrated that the absence of *Hes1* gene causes a premature differentiation of neural progenitor cells that are depleted before they have proliferated sufficiently to generate all neuronal and glial cell types. This, results in abnormalities in brain development such as small and deformed brain structures[19,25].

From these evidences, has been hypothesized that the role of the oscillations of *Hes* genes is to maintain the correct timing of differentiation process[19,26] and to lead to heterogeneous responses of cells even under the same environmental cues.

2.2 – Protein structure and mode of action of Hes family members

The seven genes of Hes family (*Hes1* to Hes7) are the mammalian orthologous of Drosophila hairy and Enhancer of split (E(spl)). These genes encode for the basic helix loop helix (bHLH) type transcriptional repressors[27]. In addition to this domain, they contain other two conserved

regions: the orange domain located just at C terminal to the bHLH domain followed by a sequence of four amino acids (Trp-Arg-Pro-Trp) at the carboxyl terminus of the protein called WRPW motive (Fig 2.1).
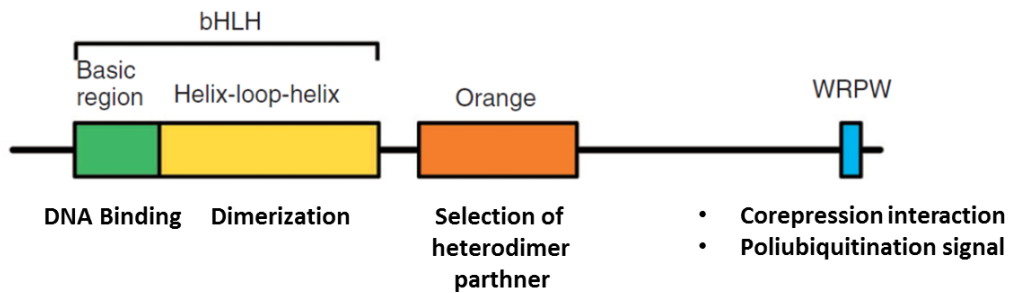
Figura 2.1 – Schematic representation of the conserved region of Hes family member and their function. In green and yellow the Basic-Helix-Loop-Helix domain; in orange the orange domain and in blue the WRPW motif. Adapted from CURRENT TOPICS IN DEVELOPMENTAL BIOLOGY, Notch Signaling. 2010

Hes proteins act as transcriptional repressors forming homodimers or heterodimer to bind respectively the N box (CACNAG) or the class C site (CACG(C/A)G) through their bHLH domain, where HLH is involved in the dimerization and the basic region binds the DNA sequences. On the other hand, the repression is mediated by the recruiting by both the orange domain and the WRPW of the Transducin-like E(spl) (TLE) genes/Groucho-related gene (Grg), corepressors that likely inactivate the chromatin by histone deacetylation[28,29].
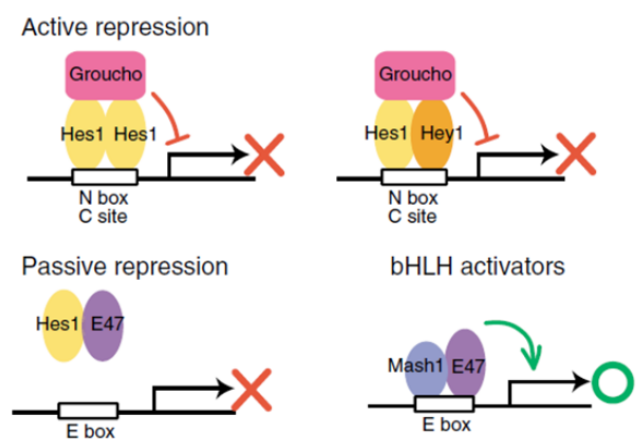
Figure 2.2 – Hes factors mode of action. **Active repression:** Hes factors bind to the N box or class C site by forming homodimers (left panel) or heterodimers with Hey1 (right panel) and actively repress transcription by interacting with co-repressors, such as Groucho homologs. **Passive repression**: Hes factors form non-DNA- binding heterodimers with bHLH activators such as E47 and inhibit transcriptional activation. Adapted from Kobayashi et al 2014

This process that is called active repression, is more efficient when Hes factors form heterodimers through their orange domain with other bHLH repressors, such as Hey1 and Hey2 (Hes-related with YRPW motif1)[30]. Moreover, Hes factors inhibit the function of the bHLH activators that bind to the E-box, by forming heterodimers and preventing their binding to DNA in a process of passive repression (Fig. 2.2)[21]

2.3 – The mechanism of *Hes1* oscillations
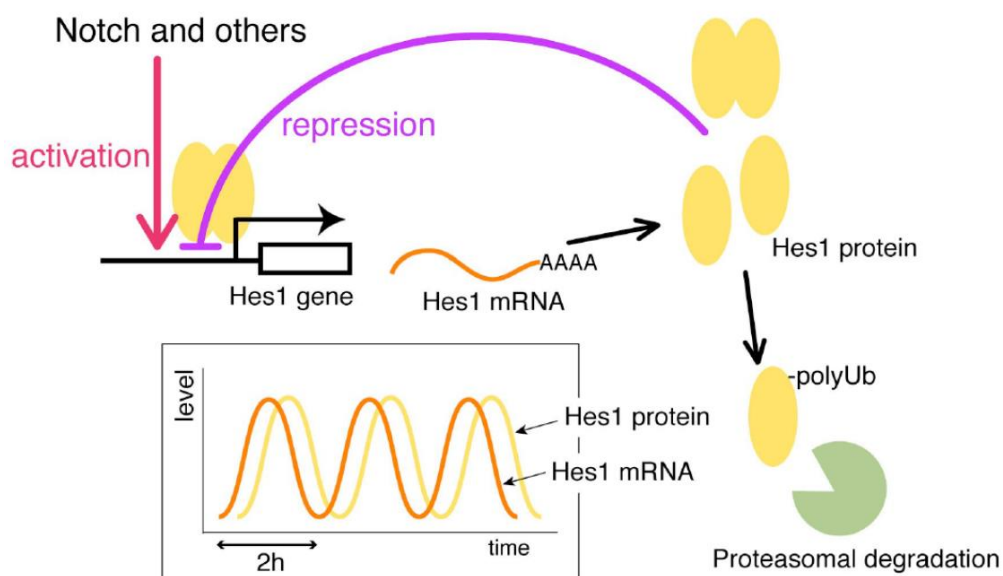
Figure 2.3 – Negative feedback mechanism underlie Hes1 oscillations. After transcriptional activation by Notch or other signaling pathway and after a certain time of delay, HES1 repressor dimerizes and binds on its own promoter region, causing the repression of its expression. The degradation of HES1 repressor via ubiquitin-proteasome system, leads to another expression cycle of *Hes1*. Adapted from Kobayashi et al 2014

Hes1 is a mammalian ultradian oscillator, it means that the period of its oscillations is shorter than 24 hours, in fact it is periodically expressed with pulses occurring about every two hours. This phenomenon has a very important biological role because it is involved in the correct development of several tissues and organs during the embryogenesis[20,31]. The mechanism proposed for this oscillator is based on a simple delayed[16] negative feedback loop and on the rapid degradation of gene products[24] (Fig.2.3).

In particular, when *Hes1* is expressed a two-steps process occurs and lead to a phase of delay in transcriptional auto-repression. In fact, once pre-mRNA is transcribed it is spliced of its three introns into a mature mRNA, this phase takes about 20 minutes[32]. Then, the mRNA is translated into the HES1 repressor, this other phase takes other 15 minutes[24]. Overall these two phases last the time (about 35 min) to generate a sufficient delay in transcriptional repression of *Hes1* gene to guarantee the onset of oscillations. When HES1 has been correctly produced it homo-dimerizes with another HES1 protein and this homodimer binds N-boxes spread on its own promoter repressing its own expression[27]. Since the gene products are highly destabilized, *Hes1* mRNA and protein are rapidly degraded and another cycle of expression can start. Has been evaluated that the half-lives of *hes1* mRNA and HES1 protein is 24.1 and 22.3 min respectively.

This instability is due to destabilization signal present on *Hes1* sequence. In particular the instability of *Hes1* protein is due to WRPW motif that works as a poli-ubiquitination signal and mediates via proteasome the protein degradation[33], whereas the *Hes1* mRNA instability could be regulated by the 3' untranslated region (3'UTR), as revealed for other Hes related mRNAs[24].

2.4 – The *Hes1* oscillations in embryogenesis

Hes genes expression is activated mainly via the Notch signaling pathway. Notch signaling is activated by direct contact of its ligands, such as DELTA or JAGGED present on the membrane of neighboring cells, called sender cells. In turn the sender cells, transmit a signal to NOTCH receptors on the surface of the receiver cell. Upon activation of Notch signaling, the NOTCH is cleaved by γ-secretase and its intracellular domain (NICD) is released from the inner part of cell membrane and it is translocated into the nucleus. Here NICD forms a complex with the DNA-binding complex RBPj/CSL, that recruits additional transcriptional co-activators and induces the expression of downstream genes, such as the genes of Hes gene family[34]. This is the canonical pathway of Notch signaling (fig 2.4).

Nevertheless *Hes1* expression is induced also by many other signaling pathways, such as fibroblast Therefore, many pathways regulate *Hes1* expression in a tissue-specific manner
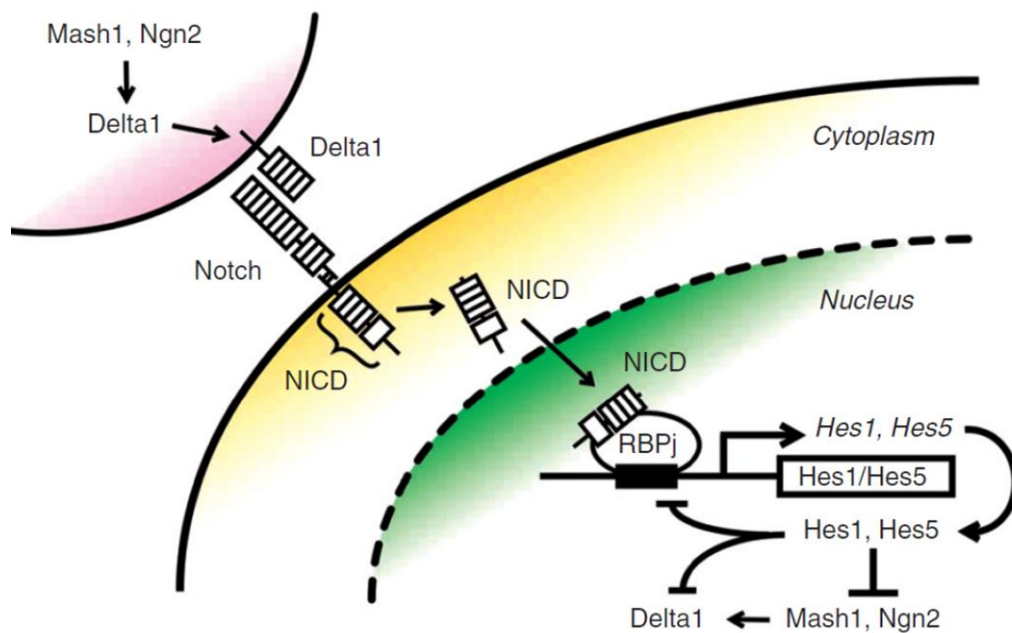
Figure 2.4 – Canonical Notch signaling pathway. When NOTCH is activated by direct contact of Dll1 on the membrane of a neighboring cell, its cytoplasmic part (NICD) is cleaved and goes into the nucleus, where the binding of RBPj complex activate the expression of several target genes, such as *Hes1*. In turn, this binding leads to repression of several genes, such as Dll1 and of differentiation program. Adapted from CURRENT TOPICS IN DEVELOPMENTAL BIOLOGY, Notch Signaling. 2010

where it plays an important role in the cell fate decision in several tissues and organs of embryos (e.g. hematopoietic stem cells, digestive organs, lung, cochlea, skeletal tissues, etc). In particular, has been shown that in embryonic stem (ES) cells and in the developing central nervous system, *Hes1* is expressed in a periodic manner giving rise to sustained oscillations with a period of 2-5 hours (ultradian oscillations has a period shorter than 24 hours).

This dynamical behavior is based on a negative feedback loop mechanisms and it is proposed to be fundamental in correct development in terms of shape, size and cell heterogeneity of the organs[20].

2.4.1 – *Hes1* oscillations in the embryonic stem cells.

Embryonic stem cells are pluripotent cells present in the inner part of blastocyst and have the ability to differentiate into multiple cell types of all three germinal layers: ectoderm, mesoderm and endoderm. When this cells receive the same differentiation stimulus they exhibit a

heterogeneous gene expression response and consequently a different cell fate decision and asynchronously differentiation into diverse cell types.
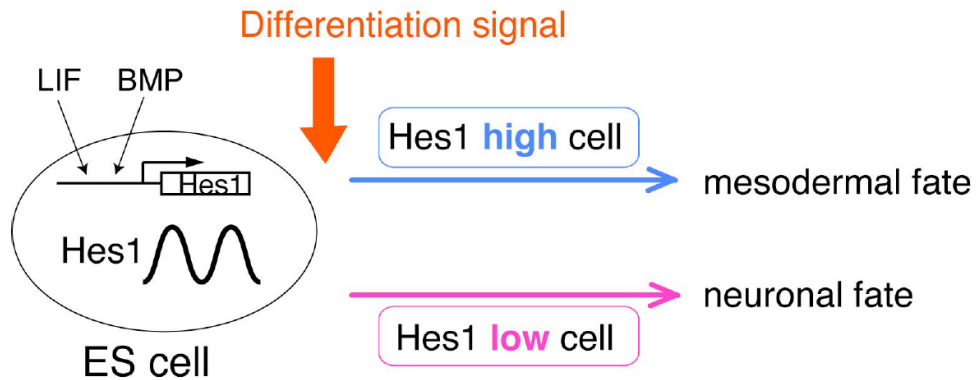
Figure 2.5 – heterogeneous response of ES cells to the same differentiation cues. The *Hes1* oscillations lead ES cells at two different initial states. When the differentiation stimulus occurs, cells that express *Hes1* at high levels tend to differentiate into mesodermal fate, vice versa cells that express *Hes1* at low levels are prone to differentiate into neurons. Adapted from Kobayashi et al 2014

Although the basic mechanism that govern this chaotic phenomenon is not completely understood, the oscillation of *Hes1* is a candidate mechanisms able to explain it. In fact, has been shown that when LIF and BMP , known inducers of *Hes1*, activate *Hes1* expression it starts to oscillate. Therefore, when ES cells receive a differentiation signal, the cells that express *Hes1* protein at low level are prone to differentiate into neuroectodermal cells, while cells expressing high levels of *Hes1* protein differentiate into early mesodermal cells (Fig. 2.5), by repressing expression of Notch ligands and cell cycle regulator genes [38].

This model has been experimentally demonstrated in knock out experiments, where *Hes1*-null ES cells display less heterogeneity in both the differentiation timing and fate choice.

Thus, from this data came up an attractive hypothesis where *Hes1* oscillations contribute to heterogeneous responses of ES cells even under the same environmental conditions[37].

2.4.2 – *Hes1* oscillations in brain morphogenesis.

In the development of mammalian nervous system, the Notch signaling pathway regulates cell differentiation by intercellular communication between two adjacent cells, leading to a

bifurcation in a cell fate decision. In fact, when the proneural factors *Mash1* and *Ngn2* are sustained expressed in the sender cell (destined to differentiate into a neuron) they induce the expression of the Notch ligand Dll1. Dll1 activates Notch signaling in neighboring cells (receiver cell), that results in the repression of proneural genes, such as *Ngn2*, and Dll1 via *Hes1*. Thereby, there is a bifurcation in cell fate choice, in which the sender cell differentiates into a mature neuron, while the receiver cell doesn't differentiate and by continues replications generate a pool of neural progenitor. Thus, Notch signaling is unidirectional, from neurons to neuronal stem cells and leads to a phenomenon known as lateral inhibition[39] (Fig. 2.6).
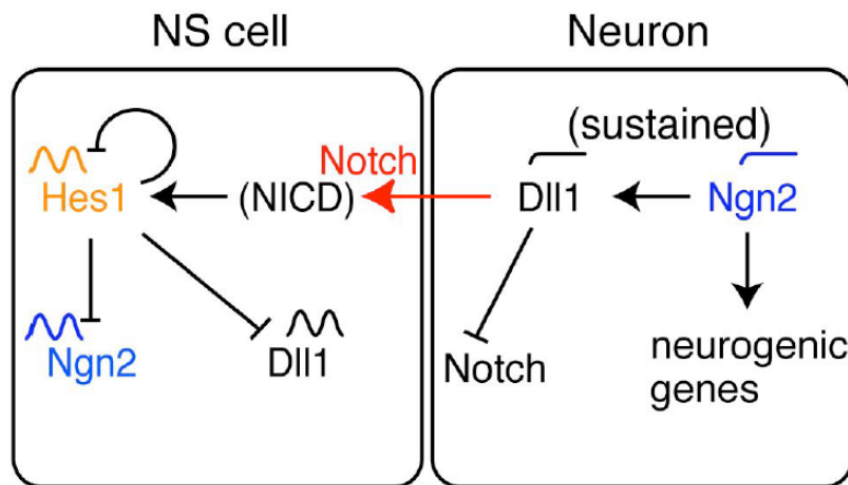
Figura 2.6 – Lateral inhibition. Notch signaling is unidirectional from differentiating neurons (right square) to neuronal stem cell (left square). Sustained *Dll1* expression prevents neurons differentiation in the receiving cell by Notch-*Hes1* pathway. Adapted from Kobayashi et al 2014

In this process in the receiver cells *Hes1* oscillates dynamically with a period of 2-3 hours and regulates the expression of *Ngn2*, *Mash1* and *Dll1* that also in turn start to oscillate[40]. This periodic expression provides another interesting strategy to maintain neural progenitor cells in their undifferentiated state (Fig 2.7).

Oscillatory expression of these genes activates only early-response genes avoiding to activate the neuronal differentiation program. When *Hes1* expression is repressed the expression of *Ngn2* and neurogenic genes becomes sustained, thereby activating late-response genes and consequently promoting the neuronal differentiation.
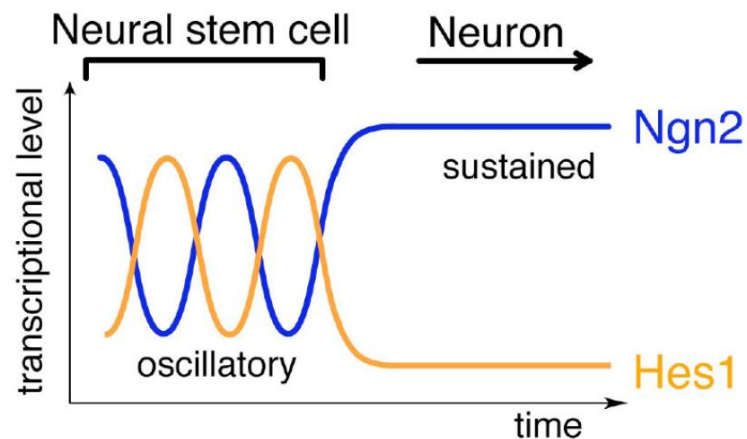
Figure 2.7 - Hes1 and *Ngn2* oscillation in nervous stem cells (NS). The levels of both *Hes1* and *Ngn2* oscillate in NS cells. When *Hes1* expression is repressed *Ngn2* expression becomes sustained and neural progenitor can differentiate into a mature neuron. Adapted from Kobayashi et al 2014

In addiction, has been demonstrated that in the developing brain the period and amplitude of *Hes1* oscillations are variable from cell to cell and from cycle to cycle resulting in an unsynchronized oscillations among cells, suggesting that these oscillations do not serve as an accurate molecular clock but to enable various responses to be individually timed[19]. Thus, these oscillations are essential for the correct formation of complex brain structures, in terms of size and neuronal cells diversity.

2.5 – Conclusions and open questions

HES1 is basic helix-loop-helix (b-HLH) transcription factor, it is expressed during embryogenesis in various regions of the embryo, such as, in the ependymal zone of central nervous system (CNS) where it is transiently expressed at a high level by the neural progenitor cells, but it decreases rapidly as neural differentiation proceeds[27]. In particular, as I mentioned before, the control of stem cell differentiation is orchestrated by very quick changes in the dynamics of *Hes1* expression. In fact, *Hes1* oscillates with a period of 2 hours and this is essential for maintenance of neural progenitors in the embryonic brain and for its healthy development.
The mechanism that has been proposed for these cell autonomous oscillations is based on a delayed negative feedback loop and on a very short protein and mRNA half-lives. Although, this

simple mechanism has been largely studied, it doesn't explain the *Hes1* behavior in terms of robustness of the period and amplitude of their oscillations. In fact, has been demonstrated that cell–cell communication stabilizes the unstable cellular oscillators through cellular coupling underlie the important role of Notch-Delta pathway and others in the onset of *Hes1* sustained oscillations[32].

 In the present work of thesis, I propose a way to elucidate which are the basal mechanisms of *Hes1* oscillations and if a simple delayed negative feedback loop is able to give raise robust oscillations of HES1 repressor.

Chapter 3 - Quantitative characterization of the *Hes1* oscillator

This chapter concerns the quantitative characterization of regulatory sequences determining *Hes1* gene expression. I experimentally identified dose-response curve of the endogenous *Hes1* promoter sequence and mathematically modelled it by a Hill function. I then performed time-lapse experiments in order to quantify the effects on mRNA stability of the *Hes1* 3'untranslated region which I cloned downstream of a reporter protein driven by an inducible promoter.

3.1 - Introduction

HES1 repress its own transcription by a negative feedback mechanism of autoregulation, and thanks to its N-terminal b-HLH domain binds multiple N-box elements (CACNAG) present on its own promoter and in this way repress its own transcription[41][21].The simplest model proposed to explain *Hes1* oscillations is based on a delayed negative feedback loop, in which HES1 after a delay caused by their introns splicing, binds its own promoter and represses its own expression.

Mathematically, this model can be described as a Goodwin oscillator, where there is one gene that is repressed by its own gene product. The Goodwin oscillator can be modeled by the following Ordinary Differential Equations (ODEs):

$$\frac{dX}{dt} = \beta_1 \left(\frac{K^n}{K^n + Z^n} \right) - (\alpha_1 X) + \gamma \tag{3.1}$$

$$\frac{dY}{dt} = (\beta_2 X) - (\alpha_2 Y) \tag{3.2}$$

$$\frac{dZ}{dt} = (\beta_3 Y) - (\alpha_3 Z) \tag{3.3}$$

In this system of three equations, each one represents the variation in the amount of a different molecular species over the time. Specifically, X describes the changes in pre-mRNA concentration, Y represents the changes in the amount of the mature mRNA, and Z describes the changes in the quantity of the mature protein.

Regarding the model parameters: alpha1 is the maturation rate of the *Hes1* pre-mRNA into mRNA, alpha2 is the mRNA degradation rate and alpha3 the protein degradation rate. A Hill function describes the repressive effect of the *Hes1* protein (Z) on its expression (X), where β1 is the maximum transcriptional rate of the promoter, K is the amount of active transcription factor (*Hes1*) in order to achieve half of the maximum transcriptional rate, and n is the Hill coefficient that represents the cooperativity of the binding between *Hes1* protein and its promoter. The parameter beta2 represents the maturation rate of the pre-mRNA (it should have the same value as alpha2 but I kept it different to allow for deviations from an ideal model), and beta3 represents the translation rate.

Since kinetics parameters describing *Hes1* protein can be derived from literature (i.e. alpha3 and beta3), I decided to focus my efforts on the identification of the parameters describing the promoter activity (i.e. the Hill function) and the mRNA degradation. Indeed, the most important factors underlying *Hes1* oscillations are the strong and non-linear repression of the promoter and the rapid degradation of *Hes1* protein and mRNA that avoid the accumulation of these two products in the cell. In contrast to *Hes1* protein, whose destabilization signal has been identified (WRPW motif)[33], for the *Hes1* mRNA a clear destabilization signal has not been yet identified.

Usually the 3' Untranslated region of a gene contains signals defined as AU rich elements (ARE) responsible of mRNA instability. Surprisingly, the *Hes1* 3'UTR does not contain any consensus sequence for I and II class ARE, but it is characterized by a high percentage of A and T. Therefore, to understand if this sequence is implicated in the mRNA destabilization, I addressed this issue by investigating the ability of this sequence to reduce the Half-life of the mRNA a generic gene.

3.2 - *Hes1* promoter characterization

In order to quantitatively characterize the promoter region of *Hes1* gene, I carried out a dose response curve in which I observed the response of *Hes1* promoter to increasing amounts of HES1 repressor. I analyzed the mouse *Hes1* promoter (pHes1) the genomic region of 2976
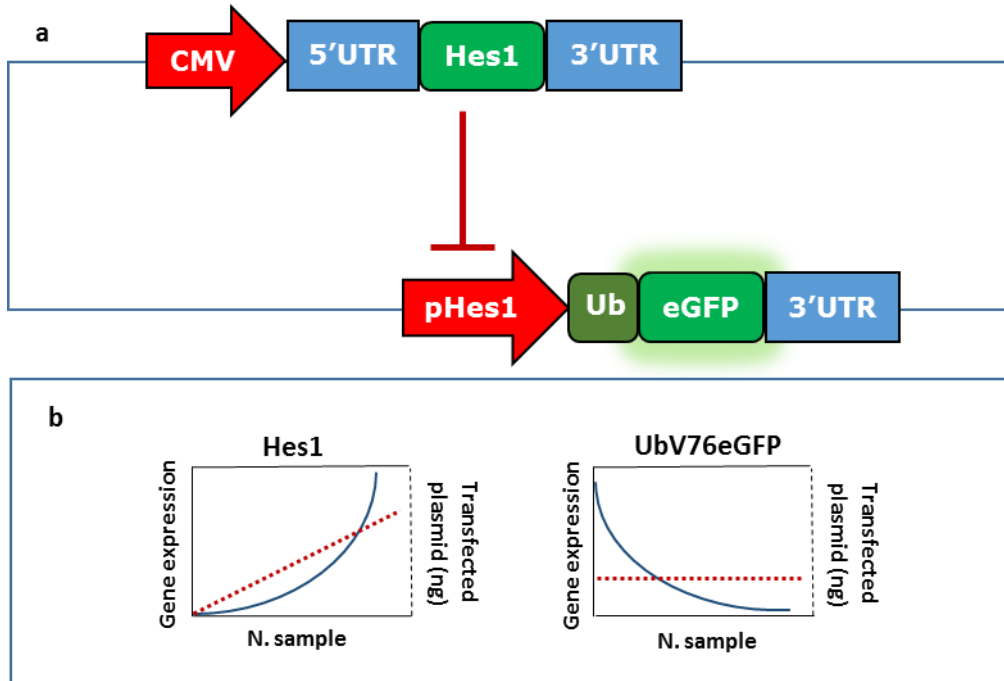
Figure 3.1 - Schematic representation of the experimental design. **(a)** Transfected gene network used to carry out the dose response curve of *Hes1* promoter. The network is composed by two plasmids, one expressing for the HES1 repressor and second plasmid expressing for a destabilized green fluorescent protein under the control of *Hes1* promoter region. **(b)** Schematic representation of the transfected amount of the two plasmids and the respective readout of the gene expression.

bp upstream of the *Hes1* ATG (-2820 to -24) that was shown to contain sites for both NOTCH induction and HES1 negative feedback.[32] In particular, I cloned downstream of the pHes1 genomic region a gene reporter expressing a destabilized Green Fluorescent protein (Ub^{V76}eGFP) and the *Hes1* 3'UTR as shown in Fig. 3.1. To repress this construct, I used a plasmid carrying the coding sequence (CDS) of *Hes1* under the control of the constitutive promoter of the Cytomegalovirus (CMV promoter). As a negative control, I used a plasmid constitutively expressing the Tetracycline Trans-activator (TTa), a bacterial transcription factor. I transfected these two plasmids in a CHO K1 cell line, using for each point of the dose-response curve a fixed amount of the plasmid carrying the promoter region and increasing amount of the plasmid expressing for HES1 repressor (Fig. 3.1). In order to maintain the total amount of the

transfected DNA equal for each transfection mix, I balanced each reaction with the right amount of the empty plasmid pcDNA3.1.

After 24 hours from transfection, a time interval needed to let to Ub^{V76}eGFP reach its steady state expression level, the samples were collected and analyzed at both protein and mRNA level. I performed cytofluorimetric analysis (Fig. 3.2) and real-time quantitative PCR (qRT- PCR) (Fig 3.3) to quantify fluorescence and mRNA levels of the reporter gene for each concentration of the HES1 repressor.
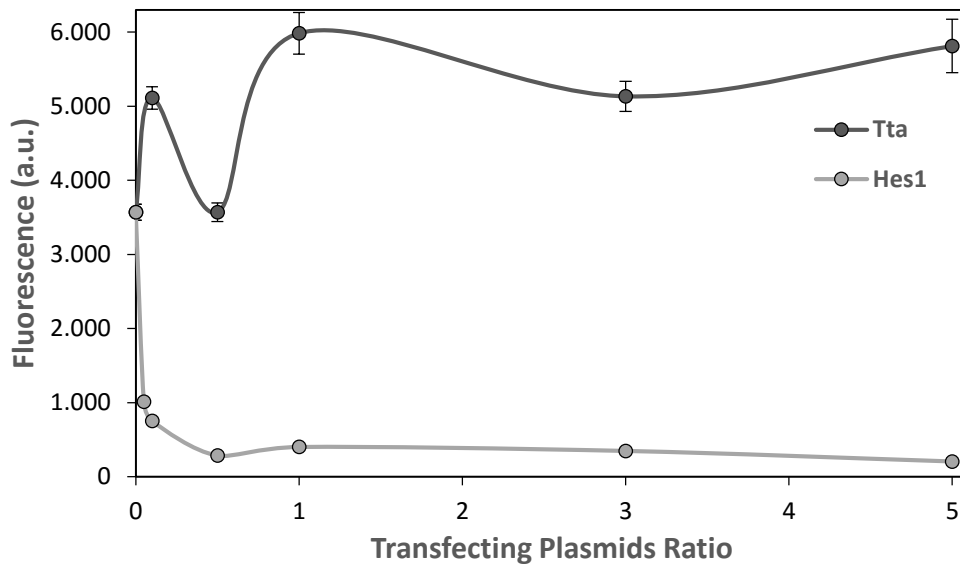
Figure 3.2 - Dose response curve of *Hes1* promoter obtained by cytofluorimetric analysis. X axes: ratios of the transfected plasmids (repressor/reporter); Y axes: fluorescence values of Ub^{V76}eGFP. The light gray line is the dose response curve of *Hes1* promoter when using the HES1 repressor. The black line is the dose response curve of the *Hes1* promoter co-transfected with the Tetracycline Trans-activator (TTa) a bacterial and non-specific transcription factor (Negative control).

As shown, in Fig. 3.2 and Fig. 3.3, I obtained a very steep dose response curve that indicates a strong response of the promoter to very low levels of the repressor. In particular, by fitting the Hill function model to mRNA expression data in Fig. 3.3, I identified the model parameters, reported in table 3.1 and I found that this curve is well described by a highly cooperativity Hill's function. Specifically, from Equation (3.1) assuming the system is at steady-state, we can write:

$$x = \beta \cdot \left(\frac{K^n}{K^n + Z^n} \right) + \gamma \qquad (3.4)$$

where $\beta = \frac{\beta_1}{\alpha_1}$ and $\gamma = \frac{\gamma}{\alpha_1}$

This Hill function was fitted to the data in reported in figure 3.3 obtaining in this way the parameters values shown in table 3.1.
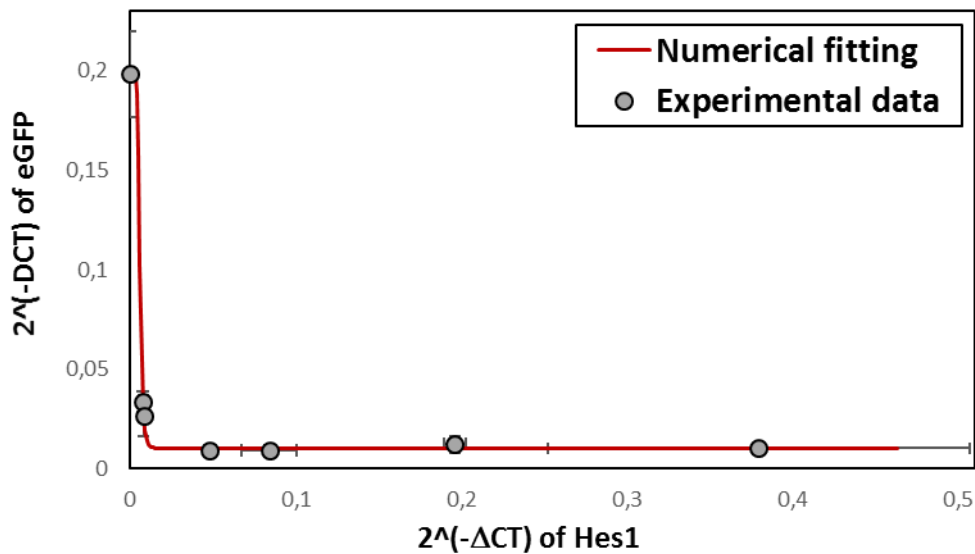
Figure 3.3 - Numerical Fitting of the dose response curve of *Hes1* promoter. Plot of the dose response curve. X axes: values of the transcriptional levels of *Hes1* repressor; Y axes: values of the transcriptional levels of the $Ub^{V76}eGFP$; The gray dots are the experimental data; The red line is the numerical fitting of the equation 3.4 to the data.

Table 3.1 – Parameters identified after the fitting procedure: are reported the parameters values describing the *Hes1* promoter repression as well as the Error Sum of Squares (**SSE**) of the fitted curve with experimental data

Parameter	Description	Fitted value
n	Hill's coefficient	7,35976
K	Concentration to achieve half of the maximal repression [a.u]	0,005959
	SSE	6,60918 10^{-06}

This result matches very well with the mono-dimensional bifurcation analysis in Fig 3.4, which was obtained with the model of the *Hes1*-Goodwin oscillator, as described by the equations 3.1, 3.2 and 3.3 with parameter reported in literature.

In particular, I studied how the equilibrium points of my system changed for variations of the parameter n (Hill's coefficient). In other words, what are the Hill's coefficient values needed in order to obtain oscillations of *Hes1* in its natural setting based on a negative feedback loop? From these analyses I found that oscillations can occur only for n > 2.
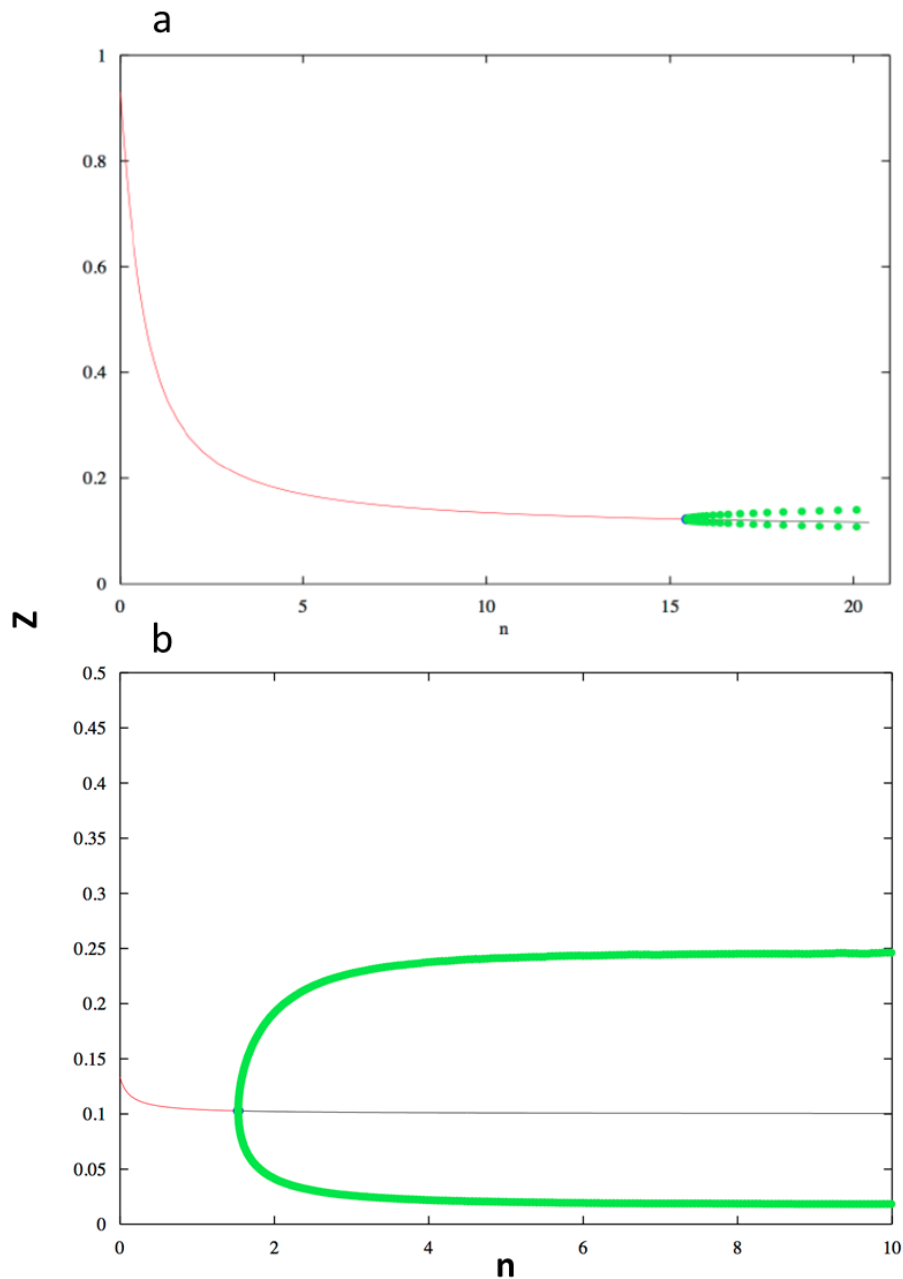
Figure 3.4 – **1-Dimensional bifurcation analysis for a general Goodwin oscillator for the Hill's coefficient (n).** The red lines represent a stable steady state, the black line is an unstable steady state, the green dots are the limit cycle whereas the distance between two green dots on the same Y axes represents the amplitude of the oscillations. (a) bifurcation diagram for the model with the linear degradation term (Equations 3.1 - 3.2 - 3.3). (b) bifurcation diagram for the model with the non-linear degradation term.

3.3 - The 3' Untranslated region of *Hes1* is a destabilizing sequence

For a biological oscillator the degradation rates of the protein and of the mRNA are very important, because a short half-life avoids the accumulation of the gene products inside the cell and allows to the promoter to initiates another transcriptional cycle.

Since the signal sequence responsible for protein degradation has already been identified, I focused my efforts on the identification of the ones responsible for mRNA degradation. For this reason, I decided to assay the effects of the *Hes1* 3'UTR for its ability to destabilize a generic transcript.

To this end, as shown in Fig. 3.4, I produced stable monoclonal cell lines, that I called Ub^{V76}eGFP-3'UTR and that I derived from CHO cells carrying an inducible gene networks based on Tet-off system (CHO Tet-off cell), in which the Tetracycline Trans-activator (TTa), drives the expression of the destabilized reporter protein Ub^{V76}eGFP, whose mRNA has the 3'UTR of *Hes1*.
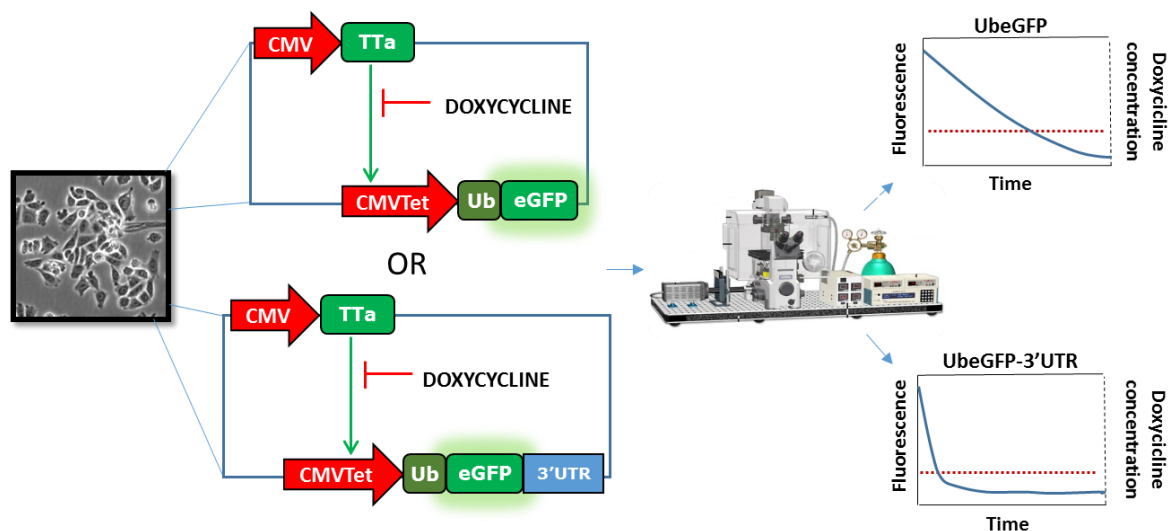
Figure 3.5 - **Schematic representation of the experimental design.** Two different monoclonal cell lines bringing two different inducible gene network based on Tet off technology. In absence of doxycycline the Tetracycline Trans-activator (TTa) drives the expression of the fluorescent gene reporter constituted by a destabilized eGFP (Ub^{V76}eGFP) in the two network respectively with and without *Hes1* 3'UTR. When doxycycline is delivered to the cells the gene network is switched off and the fluorescence decay is monitored by time lapse fluorescent microscopy.

I then performed an experiment schematized in Fig. 3.5. When Ub^{V76}eGFP-3'UTR clones were treated with doxycycline (1 μg/ml), a small molecule that binds and inhibits the TTa, the expression of the reporter protein is not active and as a results I obtain a fluorescent decay that

is function of the protein and mRNA stability. This decay was followed by time lapse fluorescent microscope and the images collected every 15' where analyzed for the mean fluorescence of the cell population by an image analysis algorithm implemented in Matlab® environment. These results were compared with a negative control constituted by a monoclonal CHO Tet-off cell lines expressing for the Ub^{V76}eGFP without the *Hes1* 3'UTR. In Figure 3.6, I reported the results of the experiments.
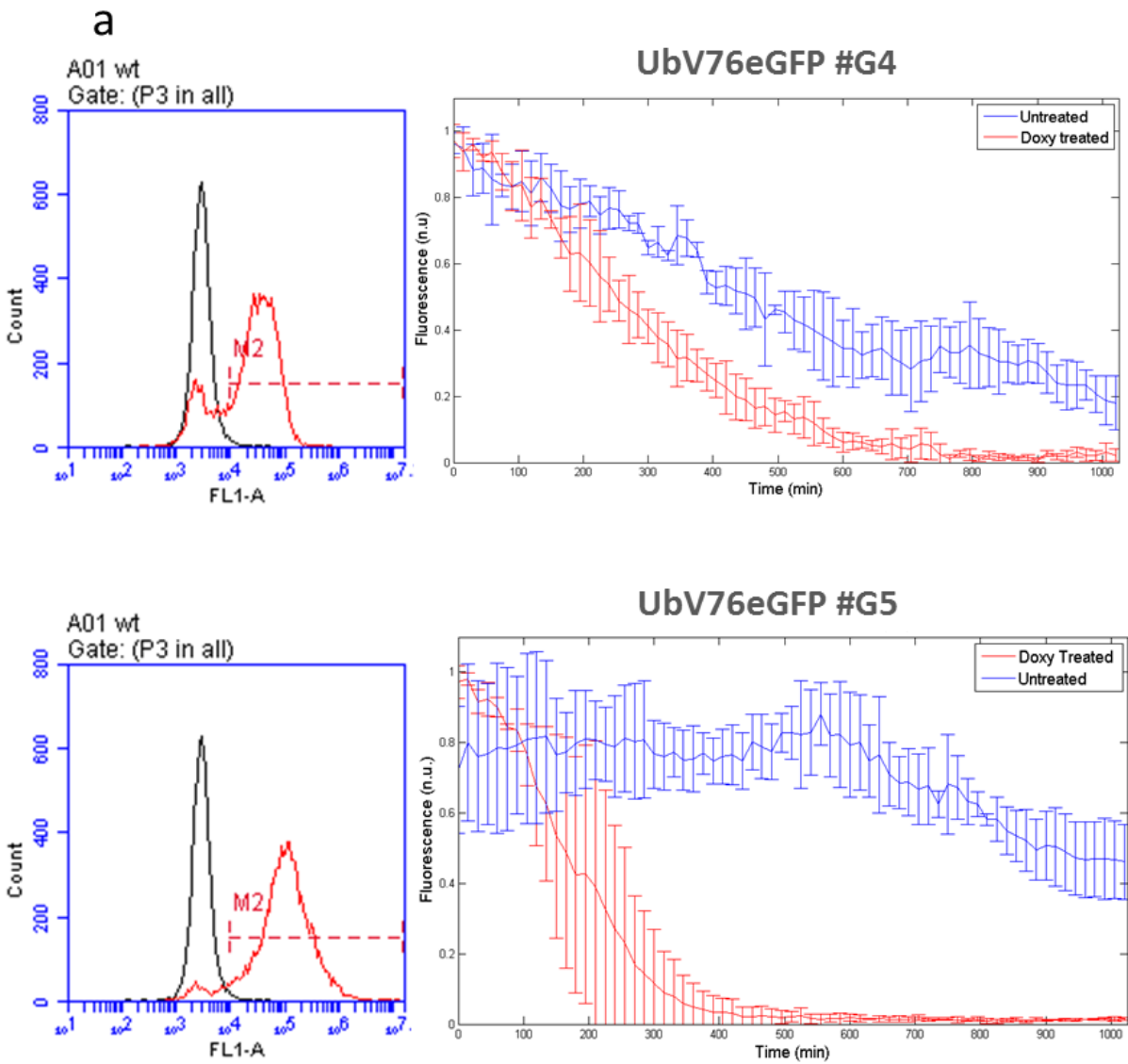
Continued on next two pages

b

A01 wt
Gate: (P2 in all)

UbV76eGFP-3'UTR #A11

A01 wt
Gate: (P2 in all)

UbV76eGFP-3'UTR #B2

A01 NT
Gate: (P3 in all)

UbV76eGFP-3'UTR #B5
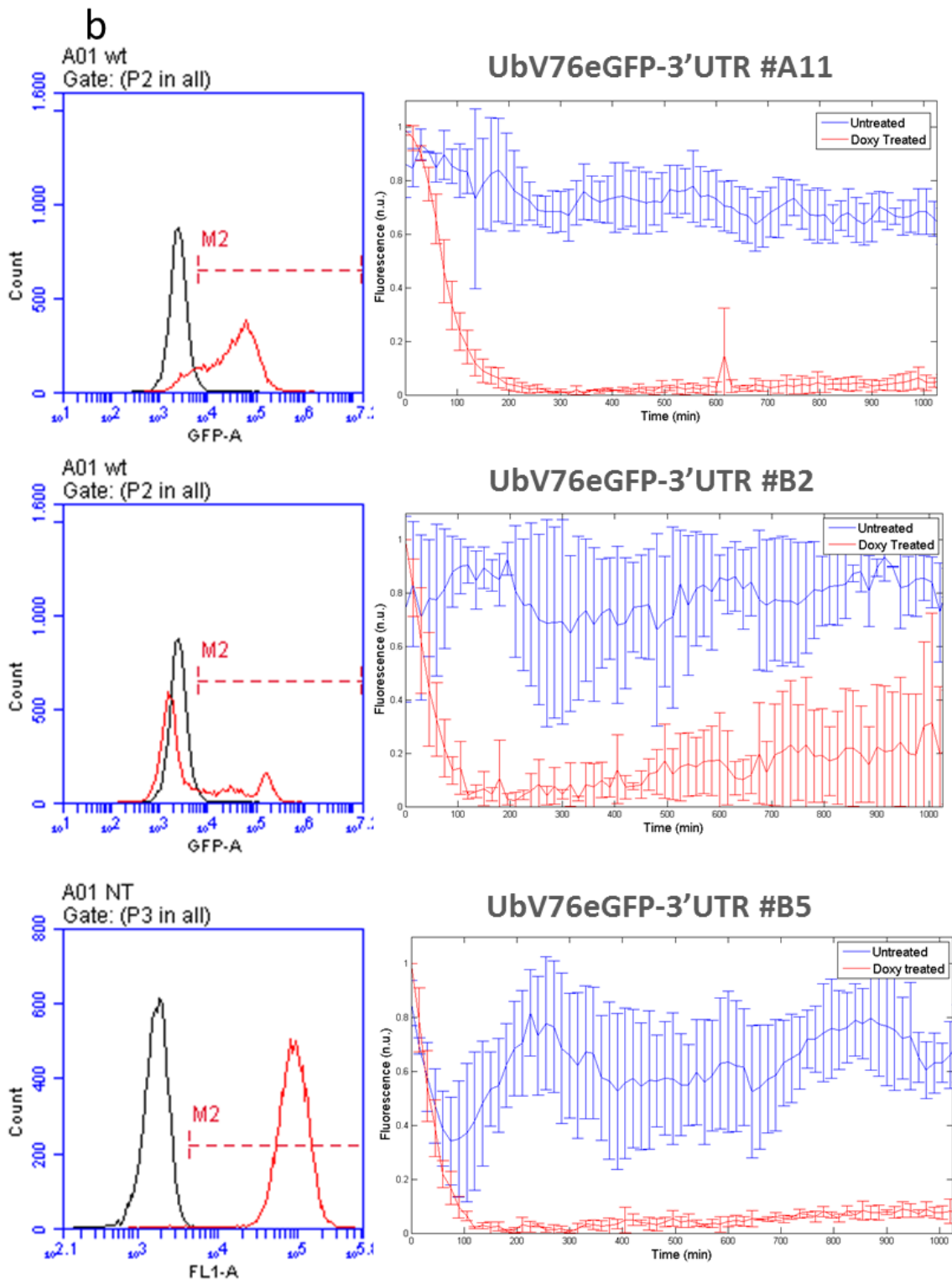
Continued on next pages

29
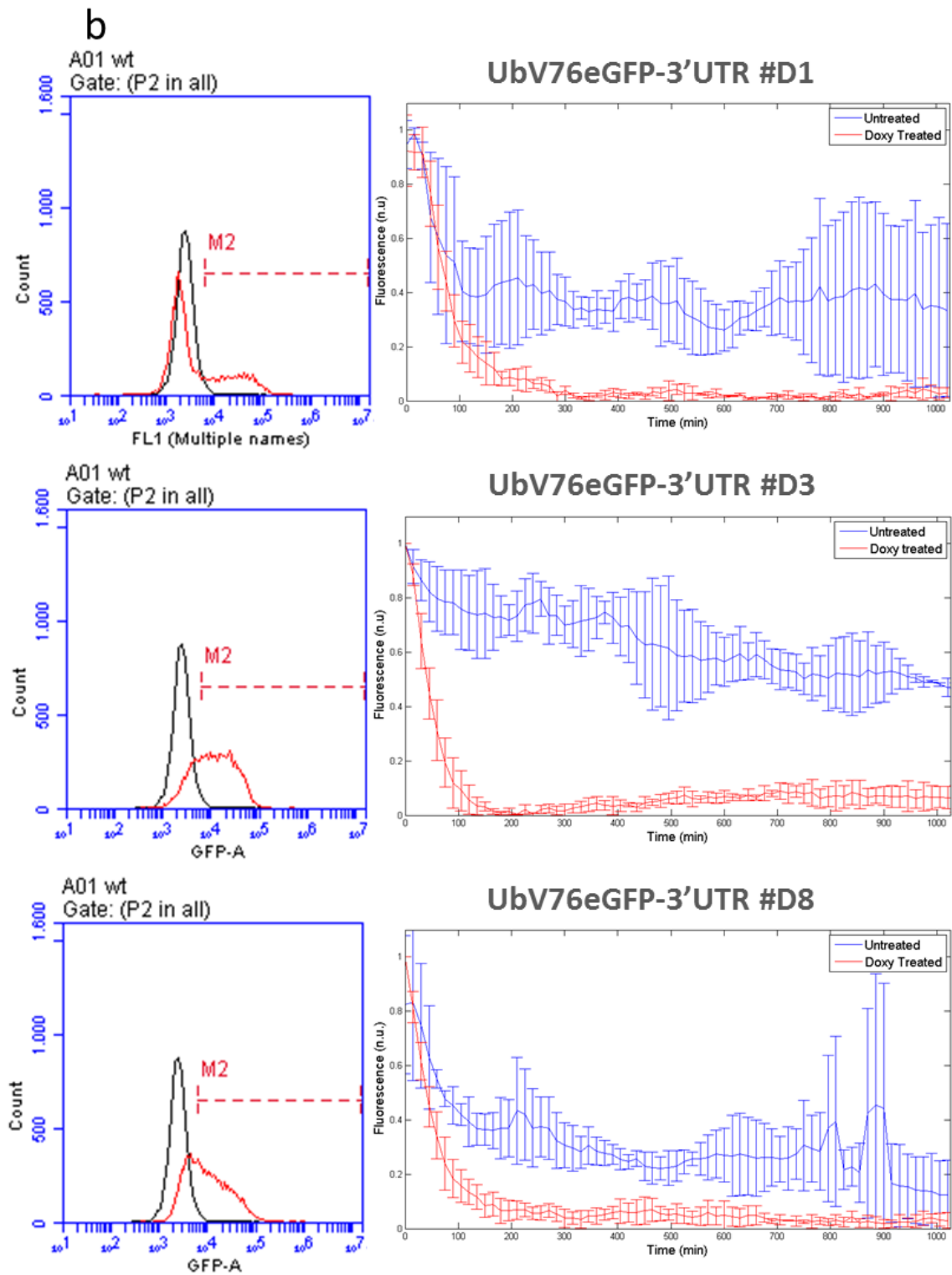
Figure 3.6 – Cytofluorimetry and time-lapse fluorescence microscopy experiments to quantify the effect on *Hes1* 3'UTR on the expression dynamics. The indicated monoclonal cell populations were treated at time zero with docycylcine (1ug/ml) to repress the reporter expression. **(a)** Monoclonal populations without the *Hes1* 3'UTR **(b)** Monoclonal populations carrying the *Hes1* 3'UTR. On the left side the histograms of the distribution of the fluorescence in each monoclonal cell population. On the right side the plots of the fluorescent decays of each monoclonal cell population following doxycycline treatment.

Overall, I obtained six functional clones carrying the gene network with the 3'UTR and two functional clones without (Fig. 3.6). Since these clones were produced by random insertion of the reporter gene I obtained several monoclonal population carrying our inducible circuits integrated inside the host genome in different copy number, different genomic loci, and with different portions. For these reasons these monoclonal cell lines shown a high dynamic variability (Fig. 3.6) depending by the three variable explained before.

Therefore, the results in figures 3.6 were mediated (Fig. 3.7) and they clearly show that the UbV76eGFP-3'UTR clones are characterized by a quicker fluorescent decay than the negative control, indicating that the 3' untranslated region of *Hes1* is the destabilization signal responsible for the rapid mRNA degradation.
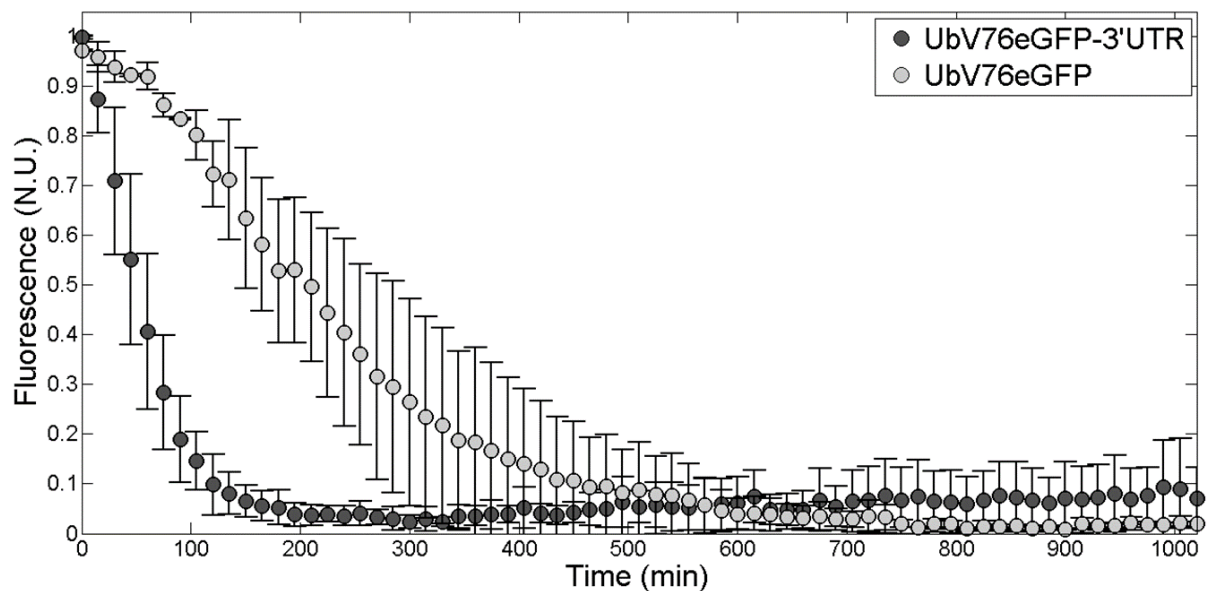
Figure 3.7 - Time-lapse fluorescence microscopy experiments of the average of the fluorescent decay of the monoclonal cell line harboring the two gene network: In dark gray da data for the network expressing Ub[V76]eGFP-3'UTR mRNA and in light gray for Ub[V76]eGFP

In order to estimate the mRNA half-life, which I did not measure directly, I first estimated the protein half-life of the reporter Green Fluorescent protein (Ub[V76]eGFP) in my cellular setting. This protein has been previously described to have a half-life of few minutes[3]. To this end, first I transfected CHO cells with a plasmid that constitutively express Ub[V76]eGFP than, at time zero I treated these cells with cycloheximide (1ug/ml) a protein synthesis

31
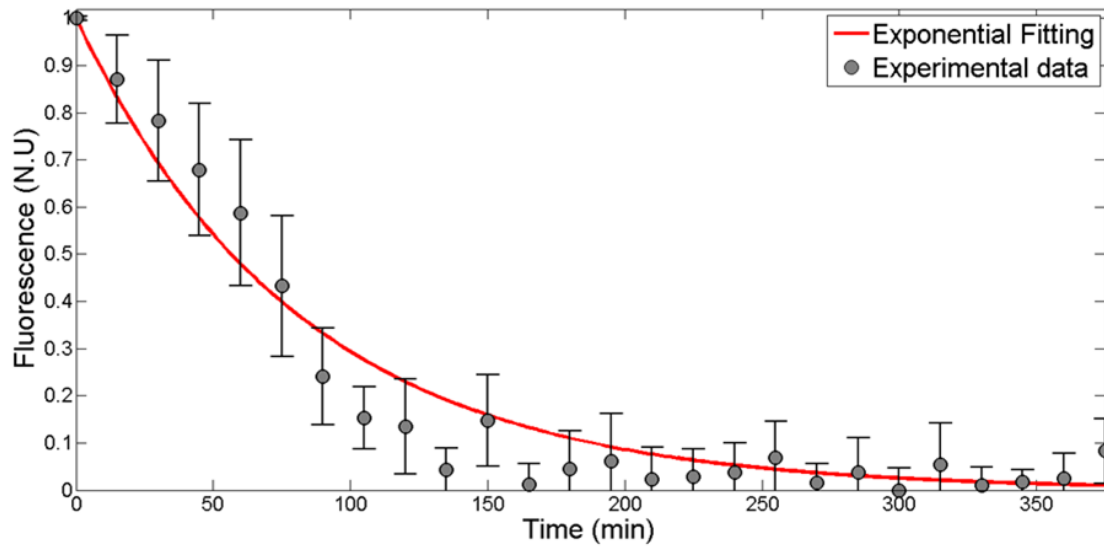
Figure 3.8 - **Half-life of the destabilized green fluorescent protein Ub^{V76}eGFP.** At time 0 cells were treated with cyclohexamide (1ug/ml) and ells were sampled at 15 minutes interval via time lapse fluorescent microscopy. X axis: time; Y axes: normalized fluorescent values. The gray dots are the experimental data; the red line is the numerical exponential fitting of the data. The estimated half-life of the protein is 56 min.

inhibitor, in order to stop the production of the fluorescent protein. Then I followed and quantify the fluorescent decay of Ub^{V76}eGFP (that is function of the Ub^{V76}eGFP stability) by time lapse fluorescent microscopy platform shown in figure 3.5.

The experimental data were fitted to an exponential curve $\mathbf{y} = \mathbf{e}^{(\alpha_2 t)}$ and the degradation coefficient α_2 was used to obtain the half-life $\left(\tau\frac{1}{2}\right)$ of the Ub^{V76}eGFP protein: $\tau\frac{1}{2} = \frac{ln2}{\alpha_2}$ (Fig 3.8 and Table 3.2).

Table 3.2 – Identification of the protein degradation rate and protein half-life for Ub^{V76}eGFP after fitting procedure

Parameter	Description	Value
α_2	Ub^{V76}eGFP protein degradation rate [min^{-1}]	0.01226
$\tau_2\frac{1}{2}$	Ub^{V76}eGFP protein Half-life [min]	56.53729'
	R-square	0.9394

Finally, in order to estimate the mRNA half-life, I used the following dynamical model:

$$\frac{dx}{dt} = \beta_1 - \alpha_1 x \qquad \beta_1 = 0 \qquad (3.5)$$

$$\frac{dy}{dt} = \beta_2 x - \alpha_2 y \qquad \alpha_2 = 0.01226 \text{ min}^{-1} \qquad (3.6)$$

The equations 3.5 and 3.6 are referred to the mRNA and protein concentration over the time respectively. This mathematical model describes the dynamics of the mRNA (x) and protein (y) products when doxycycline is added to the cells, in fact in the equation 3.5 the production rate β_1 is considered to be equal to zero. Solving equations. 3.5 and 3.6 I obtained that

$$y(t) = c_1 e^{-\alpha_1 t} + (1 - c_1) e^{-\alpha_2 t} \qquad (3.7)$$

Then, as shown in Figures 3.9 and 3.10, I fitted the experimental data to the equation 3.7 and I obtained the values of the parameters, reported in Table 3.3 and 3.4, by using the optimization Matlab Genetic Algorithm (GA)[42].
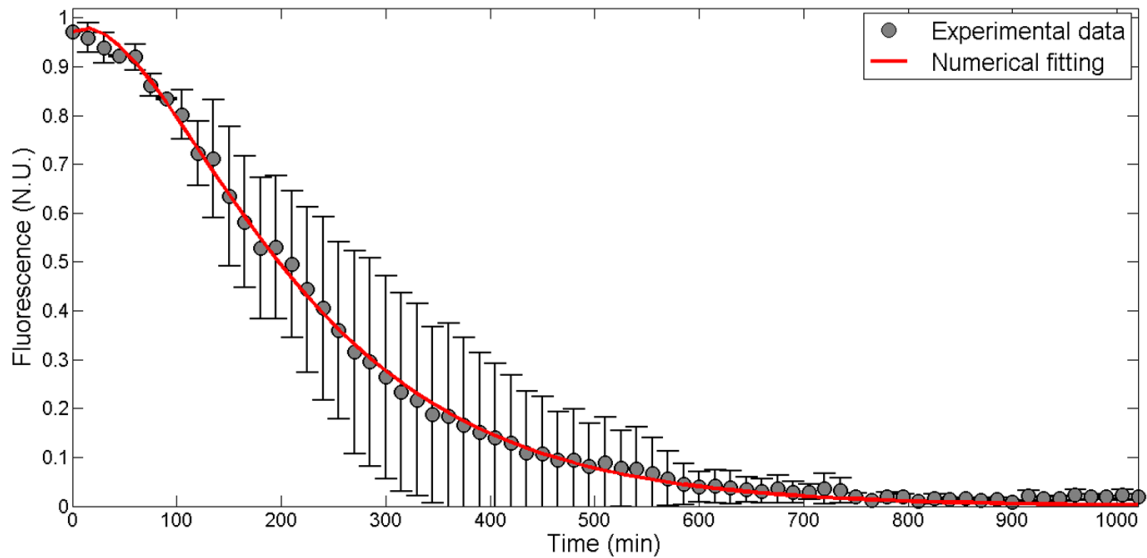
Figure 3.10 - **Numerical fitting of the equation 3.7 to the experimental data of negative control clones.** The gray dots are the experimental data obtained mediating each point of the fluorescent decay across the Ub^{V76}eGFP clones. The red line is the numerical fitting of the equation 3.7. X axes: time in min; Y axes: Normalized value of the fluorescence

Table 3.4 - **Identification of the system parameters of the equations 3.5 and 3.6 after fitting procedure with the data of negative control clones.** Are identified the protein production rate β_2, the mRNA degradation rate α_1 and mRNA Half-life as well.

Parameter	Description	Value
β_2	Protein production rate of Ub^{V76}eGFP [min^{-1}]	0.01247
α_1	mRNA degradation rate of Ub^{V76}eGFP [min^{-1}]	0.00670
$\tau_1 \frac{1}{2}$	mRNA Half-life of Ub^{V76}eGFP [min]	103.45480
	SSE	0.01135

Since the protein production rate β_2 is equal for both system carrying $Ub^{V76}eGFP$ without 3'UTR and with 3'UTR, I set β_2 equal to 0.01247. Therefore, for the system expressing $Ub^{V76}eGFP$-3'UTR only the parameter α_1 was identified.
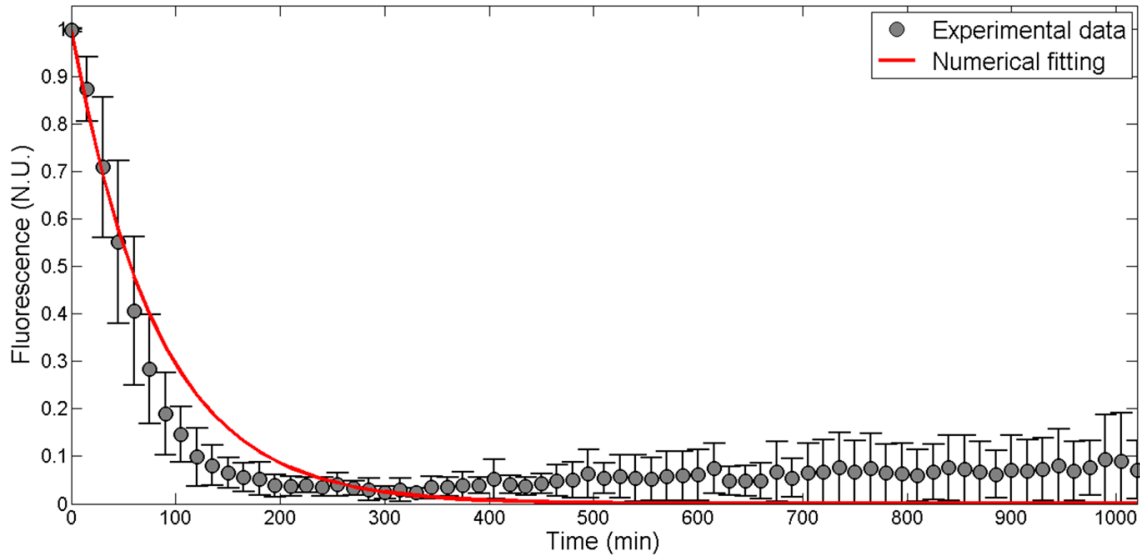
Figure 3.9 – Numerical fitting of the equation 3.7 to the experimental data of $Ub^{V76}eGFP$-3'UTR clones. The gray dots are the experimental data obtained mediating each point of the fluorescent decay across all the $Ub^{V76}eGFP$-3'UTR clones. The red line is the numerical fitting of the equation 3.7. X axes: time in min; Y axes: Normalized value of the fluorescence

Table 3.3 - Identification of the system parameters of the equations 3.5 and 3.6 after fitting procedure with the data of $Ub^{V76}eGFP$-3'UTR clones. Are identified the mRNA degradation rate α_1 and mRNA Half-life as well.

Parameter	Description	Value
α_1	mRNA degradation rate of $Ub^{V76}eGFP$-3'UTR [min^{-1}]	28.90904
$\tau_1 \frac{1}{2}$	mRNA Half-life of $Ub^{V76}eGFP$-3'UTR [min]	0.02397'
	SSE	0.5634

The mRNA degradation coefficients α_1 were used to obtain the half-lives $\left(\tau\frac{1}{2}\right)$ of the the $Ub^{V76}eGFP$ mRNAs with and without the *Hes1* 3'UTR applying this formula: $\tau\frac{1}{2} = \frac{ln2}{\alpha_1}$.

From our analysis, it clearly results that the 3'UTR is responsible for the mRNA destabilization, in fact the half-life of the transcript carrying the 3'UTR is about 1.5'' whereas the half-life of the gene network without the 3'UTR is 103'.

Chapter 4 – Design of synthetic ultradian oscillator

In this chapter I described the synthetic gene networks that I designed to recapitulate the dynamical behavior of the *Hes1* clock. In particular, in order to figure out whether this particular mono-gene network topology is sufficient to give rise periodic expression of *Hes1*, I reconstituted a delayed negative feedback loop based on the *Hes1* autoregulation. Moreover, starting from the natural *Hes1* genomic sequence, I sequentially substituted its cis-regulatory elements with synthetic counterparts. Finally, I designed more complex gene networks by adding additional genes to the previous topology. This approach based on construction and deconstruction of a gene network will shed light on the mechanism underlie *Hes1* oscillations.

4.1 - The delayed negative feedback loop

Up to now the model proposed to explain the *Hes1* oscillations is based on a delayed negative feedback loop and rapid degradation of its gene products. Therefore, in order to confirm this hypothesis, I built a set of synthetic oscillators by sequentially substituting the endogenous parts of *Hes1* with their synthetic analogs. Moreover, to derive the key components of the minimal oscillator, I performed a modular dissection of the natural occurring *Hes1* gene by producing a set of constructs lacking one or more of its elements.

4.1.1 – The modular construction of a synthetic *Hes1* analog

Applying the "build it to understand it" principle I investigated whether a delayed negative feedback loop is able to generate periodic expression of *Hes1*.

For this purpose, I cloned the mouse genomic *Hes1* sequence starting from the promoter region and including the 3'UTR (Fig 4.1 a). I then selected the CHO-k1 cell line as the cellular model to study *Hes1* oscillations, because this is an orthogonal system in which the Notch-Delta pathway is not expressed. Therefore, the behavior of the reconstituted oscillator should not be affected by the cellular environment. At this point, by sequential substitution of

cis-regulatory elements of *Hes1* with synthetic analogs designed to have a specific function, I obtained a synthetic ultradian oscillator (Fig. 4.1 d).

To test the hypothesis that the *Hes1* promoter acts as a simple transcriptional "switch" shutting down its own expression, I replaced the *Hes1* promoter, with a synthetic promoter designed to be repressible by HES1.

I built the construct shown in Figure 4.1 b where the synthetic promoter (N7CMV) was cloned upstream the 5'UTR of natural gene. Therefore, while *Hes1* is constitutively expressed by the CMV portion of the promoter, the repression is mediated by one or seven N-boxes (Fig 4.2 a), representing the specific DNA binding sites for HES1, these sequences were cloned upstream the full CMV promoter sequence.

As second step, I studied the cis-regulative elements located on the *Hes1* transcript. To this end, I substituted the 5'UTR, introns and 3'UTR with synthetic counterparts (Fig. 4.1c,d).

As I demonstrated in chapter 3, the 3'UTR is responsible for the rapid mRNA degradation of *Hes1*, however other questions regarding the role of the non-linear mRNA degradation dynamics remain opened. In fact, from bifurcation analysis shown in Chapter 3.4, I found that a non-linear degradation of the mRNA facilitates the occurence of *Hes1* oscillations. To prove experimentally this hypothesis, I produced two synthetic 3'UTR carrying two different kind of destabilization signals: the class I AU rich element (ARE-I) from c-fos (Fig. 4.3 b) and class II ARE from GM-CSF (ARE-II) (Fig. 4.2 c).

These two different classes of ARE direct the rapid mRNA degradation, but with different dynamics. In particular, the ARE of c-fos mediates a more non-linear mRNA degradation than ARE sequence of GM-CSF[43]. Thus, these two sequences constitute an useful tool to experimentally study the effects on the *Hes1* oscillations of linear and non-linear mRNA degradation.

In addition, it has been demonstrated that the *Hes1* 3'UTR is bound by the microRNA-9, that controls the stability of *Hes1* mRNA and modulates *Hes1* oscillations by forming a double-negative feedback loop. Indeed, it has been shown that both miR-9 overexpression and lack of miR-9 dampens *Hes1* oscillations[44].

Figure 4.1 – Sequential substitution of the natural parts of *Hes1* gene with synthetic counterparts. **(a)** The Natural genomic sequence of *Hes1* from promoter region to 3'UTR. **(b)** Synthetic-Natural hybrid oscillator composed by the natural parts of *Hes1* gene and a synthetic promoter (N7CMV). **(c)** Hybrid oscillator with the artificial promoter sequence, two synthetic untranslated ends and a synthetic intron. **(d)** The completely synthetic oscillator.

In order to study, the dynamical behavior of my reconstituted oscillator that is based on delayed negative feedback loop, the artificial 3'UTR that I designed contains only the AU rich elements cloned upstream SV40 poly-adenylation site. In this way, I isolated the synthetic oscillator from possible binding of trans-regulatory elements.

Figura 4.2 – Consensus sequences for synthetic sequence analogs. **(a)** N-Box recognized by b-HLH domain of *Hes1*. **(b)** I class AU rich element from 3'UTR of c-fos. **(c)** II class AU rich element from 3'UTR of GM-CSF.

Introns play a very important role in the oscillatory expression of genes in mammalian cells. Indeed, it has been demonstrated that the presence of introns in Hes gene family members generates a delay essential for their oscillations. The reduction of the number of introns shortens the delay and results in a shorter period of the oscillations [16,45,32]. Moreover, it has been shown that the intron length is proportional to the period of gene expression oscillations in a synthetic oscillator[8,16,32,45]. However, it is not yet clear if this delay is caused by introns' length and therefore by transcriptional process, or it is due to introns' number and therefore to the splicing process.

Thus, I substituted the three introns present in the *Hes1* genomic sequence with only one intron formed by the fusion of the three natural occurring *Hes1* introns. In this way the oscillator harbor just one intron characterized by the same sequence and length of the natural ones.

Finally, as shown in Fig. 4.1 d, I substituted the *Hes1* coding sequence (CDS) with an artificial transcription factor, the tetracycline repressor (TetR) a bacterial transcription factor orthogonal to mammalian cells. Similar to *Hes1*, TetR homodimerises and it is characterized by a high destabilization rate.

4.1.2 – The modular dissection of *Hes1* gene

The circuits proposed so far can give us information about the role of the *Hes1* cis-regulatory elements, and they can clarify whether the dynamical behavior of *Hes1* can be explained only on the basis of a delayed negative feedback. However, other questions regarding the architecture of the minimal oscillator remain open.

To address these problems, I designed an additional set of "negative control" constructs, in which starting from the natural *Hes1* genomic region (from 5' to 3'UTR) under the control of N7CMV synthetic promoter (Fig. 4.3 a) I performed a modular dissection by producing a set of construct lacking of one or more cis regulatory elements.

First, I cut away the 3'UTR (Fig. 4.3 b) to study the role of *Hes1* mRNA destabilization on *Hes1* oscillations, then I designed a construct with a promoter lacking of the N-boxes in order to see if the N-box present in the 5'UTR is enough to mediate the repression (Fig. 4.3 c). For

the same reason, I cut away the 5'UTR (Fig. 4.3 d) in order to study the effect of the putative N-boxes that I identified by bioinformatics analysis on the CDS and the third intron of the *Hes1* genomic sequence. Finally, I eliminated also the introns to asses if the delay given by the length of *Hes1* CDS is sufficient to give rise sustained oscillations.
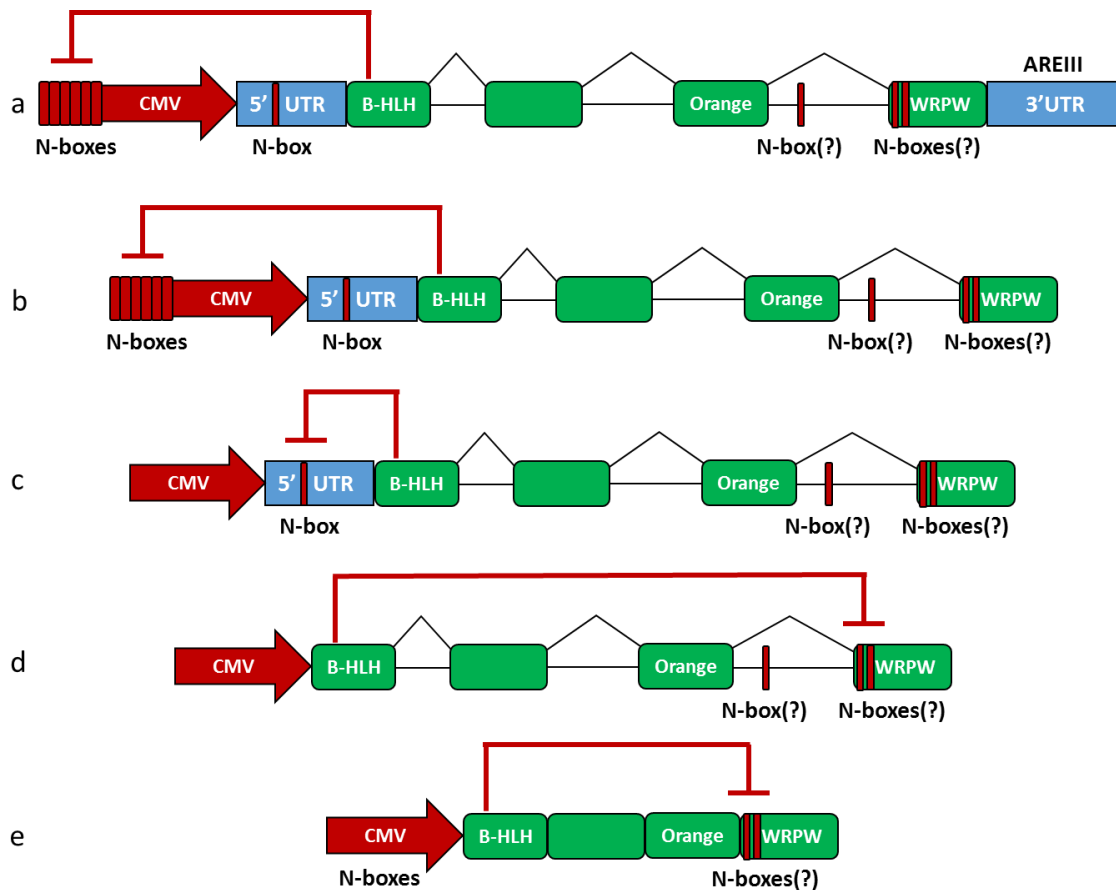
Figure 4.3 – Modular dissection of the *Hes1* gene locus. **(a)** The genomic region of *Hes1* from 5'UTR to 3'UTR expressed by the *Hes1* synthetic promoter. **(b)** Construct lacking of the *Hes1* 3'UTR. **(c)** Construct lacking of both the 3'UTR and the N-boxes on the promoter. **(d)** Construct missing of the promoter N-boxes, 3'UTR and 5'UTR. **(e)** Construct lacking of the introns.

4.2 – A more complex synthetic ultradian oscillator.

In this paragraph, I designed an inducible gene network composed by three genes: the tetracycline trans-activator (TTa), the NOTCH Intracellular domain (NICD) and a fusion gene composed by the fluorescent reporter eGFP fused in frame at the 3' of *Hes1* gene coding for the fusion protein that I called HES1-eGFP (Fig. 4.4).
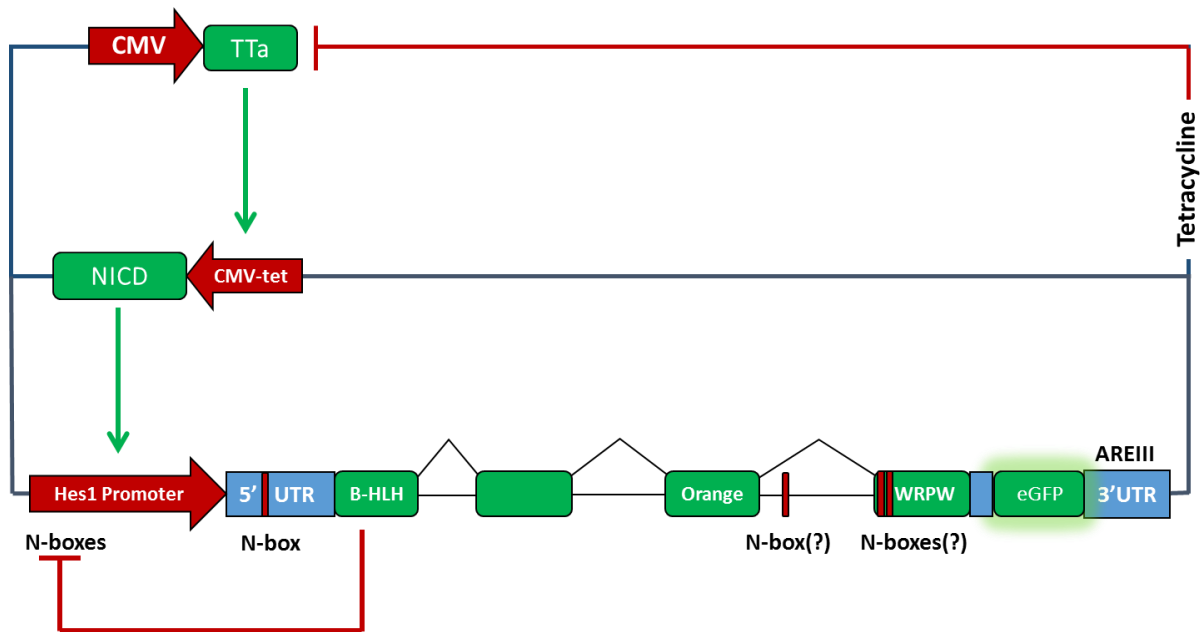
Figure 4.4 – Detailed representation of the inducible synthetic ultradian oscillator network. The inducible network is based on Tet-off technology: when cells are feed with tetracycline the circuit is switched off. The CMV-tet inducible promoter drives the expression of Notch Intracellular domain (NICD), it binds and activate the *Hes1* promoter, thus inducing *Hes1* expression. The HES1 protein then represses its own expression by binding its own promoter.

As shown in Fig. 4.4, the CMV promoter drives the expression of TTa that, in absence of tetracycline, is able to drive the expression of NICD. Conversely, NICD binds the *Hes1* promoter and triggers the negative feedback loop. When tetracycline is provided to the cells, this small molecule binds TTa and prevents its binding to CMV-Tet promoter, causing the repression of the gene network.

Finally, since in this case we use the *Hes1*-eGFP fusion protein, we can follow in single cell the expression of *Hes1* by time lapse fluorescent microscopy.

4.3 – The Smolen oscillator

The oscillators can be the components of larger networks and regulate the complex behavior of the biological systems, therefore the robustness of their oscillations is vital for the living organisms. Although the Goodwin oscillator is a good model to explain *Hes1* oscillations, it is not so robust in terms of period, amplitude and percentage of oscillating cells [4]. For this reason, I think that a more realistic model responsible for *Hes1* oscillations cannot be based simply on a delayed negative feedback loop but on a more complex genetic circuit.

To test this hypothesis, I built a gene network of two genes based on the topology of the classical Smolen oscillator (described in Chapter 1). The first gene (Activator) promotes its own transcription and that of a repressor gene, that inhibits its own transcription and that of the activator (Fig. 4.5 a).
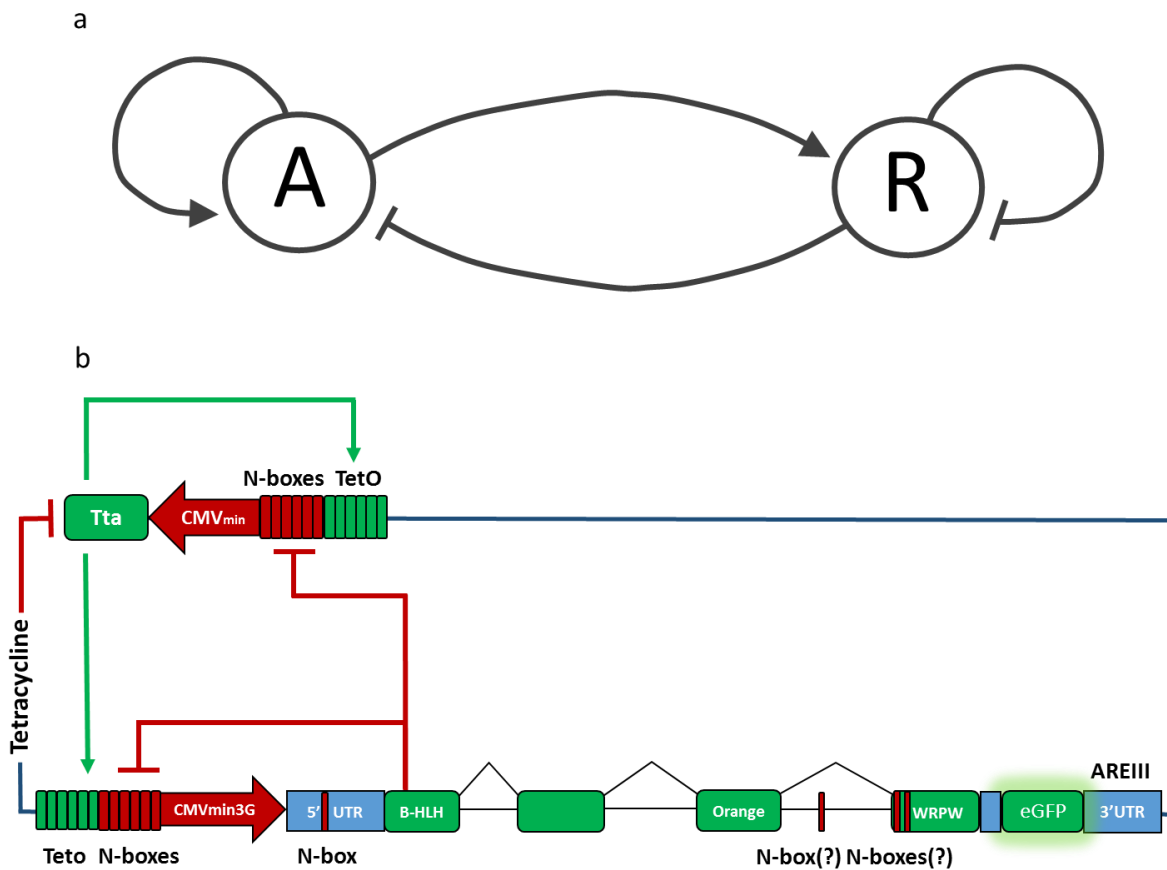
Figure 4.5 – The Smolen *Hes1* oscillator. **(a)** Network topology of the Smolen oscillator: A is the activator that activate itself and repressor R that conversely inhibits itself and A. **(b)** Detailed representation of the *Hes1* oscillator in the Smolen setting: An inducible/repressible promoter drives the expression of the Tetracycline Trans-activator (TTa) that activate itself and the *Hes1* repressor by a positive feedback loop. After a delay given by its three introns *Hes1* repress its self and TTa.

To obtain this oscillator, I designed a network of two genes repressible by tetracycline in which the activator (TTa) and the repressor *Hes1* are under the control of two hybrids synthetic promoters (inspired to p_{TRE2} and p_{TRE3G} of Clontech®)[46] carrying both the activation sites for TTa and inhibition sites for HES1 upstream of a minimal CMV promoter. In particular, the CMV minimal promoter carries seven Tet-O consensus sequences, the sequence recognized by TTa, followed by seven N-box repetitions.

Therefore, this network is repressed by tetracycline, but in absence of this molecule the TTa drives *Hes1* expression its own transcription, conversely *Hes1* represses itself and TTa by direct binding of the N-boxes and Tet-O (Fig.4.5 b).

Finally, in order to make the delay in transcriptional repression more robust, I plan to exploit the different leakiness of the two promoters. In fact, I designed the synthetic promoter expressing for the repressor with a sequence that is bound by a very low number of endogenous transcription factors[47], showing a very low basal transcriptional rate (Figure 4.6)

a

Motif Name	Position	Length	Sequence
IRF-1	197 ~ 209	13	gaaaagtgaaagt
IRF-1	239 ~ 251	13	gaaaagtgaaagt
IRF-1	281 ~ 293	13	gaaaagtgaaagt
IRF-1	323 ~ 335	13	gaaaagtgaaagt
IRF-1	365 ~ 377	13	gaaaagtgaaagt
IRF-1	407 ~ 419	13	gaaaagtgaaagt
IRF-1	449 ~ 461	13	gaaaagtgaaagt
IRF-2	197 ~ 209	13	gaaaagtgaaagt
IRF-2	239 ~ 251	13	gaaaagtgaaagt
IRF-2	281 ~ 293	13	gaaaagtgaaagt
IRF-2	323 ~ 335	13	gaaaagtgaaagt
IRF-2	365 ~ 377	13	gaaaagtgaaagt
IRF-2	407 ~ 419	13	gaaaagtgaaagt
IRF-2	449 ~ 461	13	gaaaagtgaaagt
YY1	548 ~ 567	20	gagacgccatccacgctgtt
SMAD	582 ~ 590	9	agacaccgg
IRF	198 ~ 208	11	aaaagtgaaag
IRF	240 ~ 250	11	aaaagtgaaag
IRF	282 ~ 292	11	aaaagtgaaag
IRF	324 ~ 334	11	aaaagtgaaag
IRF	366 ~ 376	11	aaaagtgaaag
IRF	408 ~ 418	11	aaaagtgaaag
IRF	450 ~ 460	11	aaaagtgaaag
Kid3	558 ~ 562	5	ccacg
DRI1	4 ~ 9	6	aattaa
IRF-7	200 ~ 206	7	aagtgaa
IRF-7	242 ~ 248	7	aagtgaa
IRF-7	284 ~ 290	7	aagtgaa
IRF-7	326 ~ 332	7	aagtgaa
IRF-7	368 ~ 374	7	aagtgaa
IRF-7	410 ~ 416	7	aagtgaa
IRF-7	452 ~ 458	7	aagtgaa
HES1	10 ~ 19	10	ggcacgagcc
HES1	32 ~ 41	10	ggcacgagcc
HES1	54 ~ 63	10	ggcacgagcc
HES1	76 ~ 85	10	ggcacgagcc
HES1	98 ~ 107	10	ggcacgagcc
HES1	120 ~ 129	10	ggcacgagcc
HES1	142 ~ 151	10	ggcacgagcc

b

Motif Name	Position	Length	Sequence
TATA	435 ~ 449	15	ctataaaagcagagc
FAC1	483 ~ 496	14	ttccacaacacttt
PEA3	521 ~ 527	7	acttcct
Nkx2-5	517 ~ 526	10	taccacttcc
HOXA13	437 ~ 442	6	ataaaa
AML2	485 ~ 495	11	ccacaacactt
HES1	9 ~ 18	10	ggcacgagcc
HES1	31 ~ 40	10	ggcacgagcc
HES1	53 ~ 62	10	ggcacgagcc
HES1	75 ~ 84	10	ggcacgagcc
HES1	97 ~ 106	10	ggcacgagcc
HES1	119 ~ 128	10	ggcacgagcc
HES1	141 ~ 150	10	ggcacgagcc
Foxj1	482 ~ 496	15	attccacaacacttt

Figura 4.6 - Transfac analysis of the synthetic promoters. (a) Leaky promoter (b) Non-leaky promoter

In this way, since I put the activator (TTa) under the control of a leaky promoter, it is rapidly expressed because in the cell there are already present endogenous transcription factors, whereas the repressor (*Hes1*) under the control of the "non-leaky" promoter, to be expressed needs the presence of the TTa protein.

Chapter 5 - Quantitative characterization of synthetic ultradian oscillators

In this chapter I analyzed in theCHO-K1 cell line the dynamical behavior of the reconstituted *Hes1* oscillator and of a subset *Hes1* synthetic analogs that I designed in Chatper 4. First I validated the biological building blocks, such as promoter and introns for their ability to perform their specific function. Then, I analyzed the dynamical behavior of the reconstituted *Hes1* in order to check whether this simple circuit is able to give rise oscillations

5.1 - Building blocks validation

In this paragraph I show the validation of two synthetic promoters to be repressible by HES1, these two promoters carry one and seven N-boxes respectively. Moreover, I validated in my cellular system the splicing process for *Hes1* pre-mRNA and for the introns ability to generate a delay in transcriptional repression.

5.1.1 – Synthetic promoter and validation

I produced and validated by dose response curve two synthetic promoters composed by the CMV promoter in which I cloned upstream one (N1CMV) or seven (N7CMV) N-boxes respectively (Fig. 5.1).
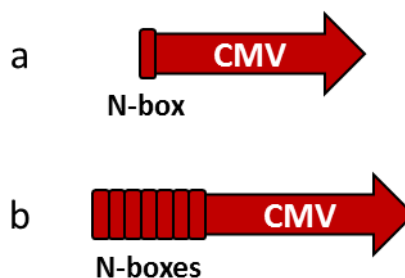
Figura 5.1 – Schematic representation of the two synthetic promoters. The red arrow is the CMV promoter the red rectangle are the Nboxes. **(a)** CMV promoter carrying one N-box (N1CMV) **(b)** CMV promoter with seven N-Box repetitions (N7CMV)

As described in section 3.2, for each point of the dose response curve, I transfected CHO K1 cells with fixed amount of the synthetic promoter driving the expression of the destabilized $Ub^{V76}eGFP$ and increasing amount of the the *Hes1* repressor. Then, at the steady state, I carried out the measurement of cell fluorescence by cytofluorimetric analysis (Fig. 5.2).

From these experiments I found that both the promoters are functional and that one N-Box is sufficient to mediate the transcriptional repression of a strong promoter. Nevertheless, for the construction of the oscillator, I decided to use the N7CMV promoter because it shows a stronger repression than N1CMV at low transfected plasmid ratios.
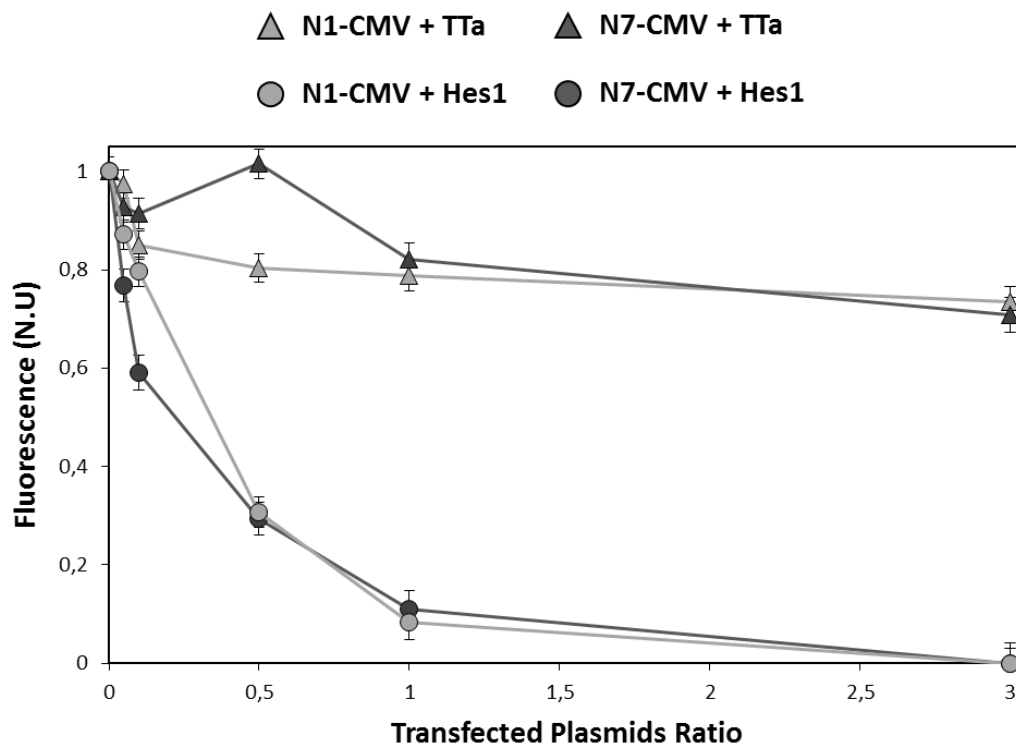
Figura 5.2 – Dose response curve of the synthetic promoters. X axes: ratios of the transfected plasmids (reporter/ repressor); Y axes: fluorescence values of $Ub^{V76}eGFP$. In light gray is the dose response curve for N1CMV promoter, in dark gray the dose response curve for N7CMV promoter. the triangles are the data for the negative control: pHes1 + TTa; the circles are the data for the experiment: pHes1 + *Hes1* CDS

5.1.2 – Splicing validation

Since I want to use the mouse genomic sequence of *Hes1* in Chinese hamster cells (CHO k1), I had to evaluate whether the splicing process for this gene happens in this cell line. For this

reason, I analyzed by gel electrophoretic assay the length of the *Hes1* transcript after transfection in CHOk1 cells (Fig 5.3).

In particular, in order to see whether *Hes1* gene is correctly spliced in our cell line, I transfected CHO k1 with the genomic sequence of *Hes1* (gHes1). After 24 hours from the transfection, I extracted the total mRNAs and I produced by retrotranscription the cDNAs. By PCR I amplified the *Hes1* cDNA spanning from the 5'UTR to the stop codon by using a specific pair of primers. Finally, I analyzed the length of the amplicon by agarose gel electrophoresis (Fig 5.3). In case of an unspliced transcript I should obtain an amplicon of 2kb otherwise an amplicon of 1Kb.

From the gel, it clearly results that that *Hes1* has been correctly spliced. Indeed in the gHes1 lane obtained by PCR from cell transfected with the *Hes1* genomic sequence, I got a clear band at 1kb (the weight of the spliced transcript) and no band at 2 kb (the weight of the spliced transcript).
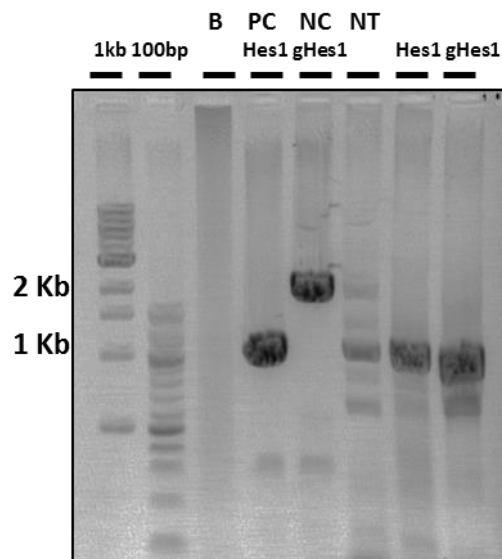
Figure 5.3 – Electrophoretic essay for Hes1 splicing validation. Agarose gel to evaluate the length of *Hes1* cDNA; from left to right: lanes 1 and 2 (1kb and 100bp): markers of molecular weight; Lane 3: water; Lane 4 (PC): amplicon from the PCR on the plasmid carrying the *Hes1* CDS; lane 5 (NC): amplicons from PCR on the plasmid carrying the genomic sequence of *Hes1*; lane 6 (NT): PCR amplification of the cDNA coming from untransfected CHO cells; lane 7 (*Hes1*): PCR amplification on the cDNA obtained by CHO cells transfected with the *Hes1* CDS; Lane 8 (gHes1): PCR amplifications of the cDNAs obtained by CHO cells transfected with the genomic sequence of *Hes1*.

Therefore, I can conclude that the genomic *Hes1* is able to splice in our cellular model.

5.2 – Reconstruction of *Hes1* oscillator in CHO cells

To assess if the delayed negative feedback loop is the mechanism driving *Hes1* oscillations, I built the N7CMV-5'UTR-gHes1-3'UTR construct composed by the genomic sequence of *Hes1* spanning from the 5'UTR to the 3'UTR under the control of the *Hes1* synthetic promoter N7CMV (Fig. 5.4 a), which I described in Chapter 4.
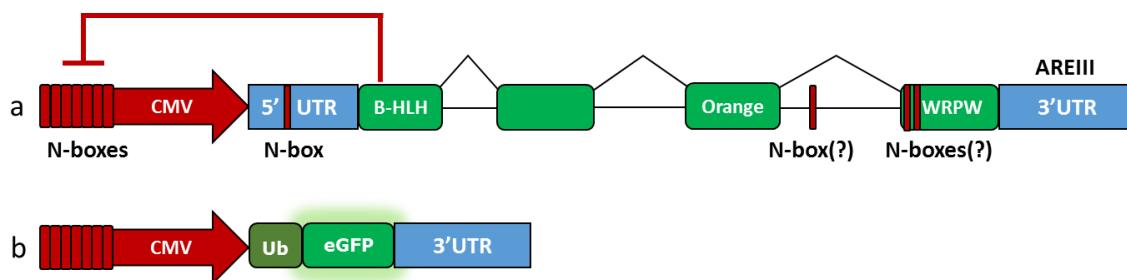
Figure 5.4 – Schematic representation of the Hes1 oscillator constructs. In red are the cis regulatory elements acting at transcriptional level; in blue the cis regulatory elements acting at mRNA level; In green the protein domains; black triangles are the introns **(a)** *Hes1* oscillator: N7CMV-5'UTR-gHes1-3'UTR **(b)** Negative control: N7CMV-Ub^{v76}eGFP-3'UTR

To analyze its dynamic behavior, I transfected this network in CHO K1 cell line where *Notch* and *Dll1* are not expressed, so we are provided with an orthogonal system where the cellular environment does not affect the reconstituted gene.

At this point in order to synchronize the cellular population, I starved the cells and to switch on the circuit I shocked them by serum treatment. I measured by RT-PCR the mRNA level of *Hes1* until 300 minutes and I obtained that in opposition to the negative control (Fig. 5.4 b) that riches the steady state, the *Hes1* oscillator show fluctuation in its expression levels.

These results suggest that a simple delayed negative feedback is sufficient to give rise periodic pulses of *Hes1*. However, the high experimental variability and the low experimental replicability suggested that my experimental approach based on transient transfections and whole population gene expression measurements is not the best approach to study oscillatory phenomena.
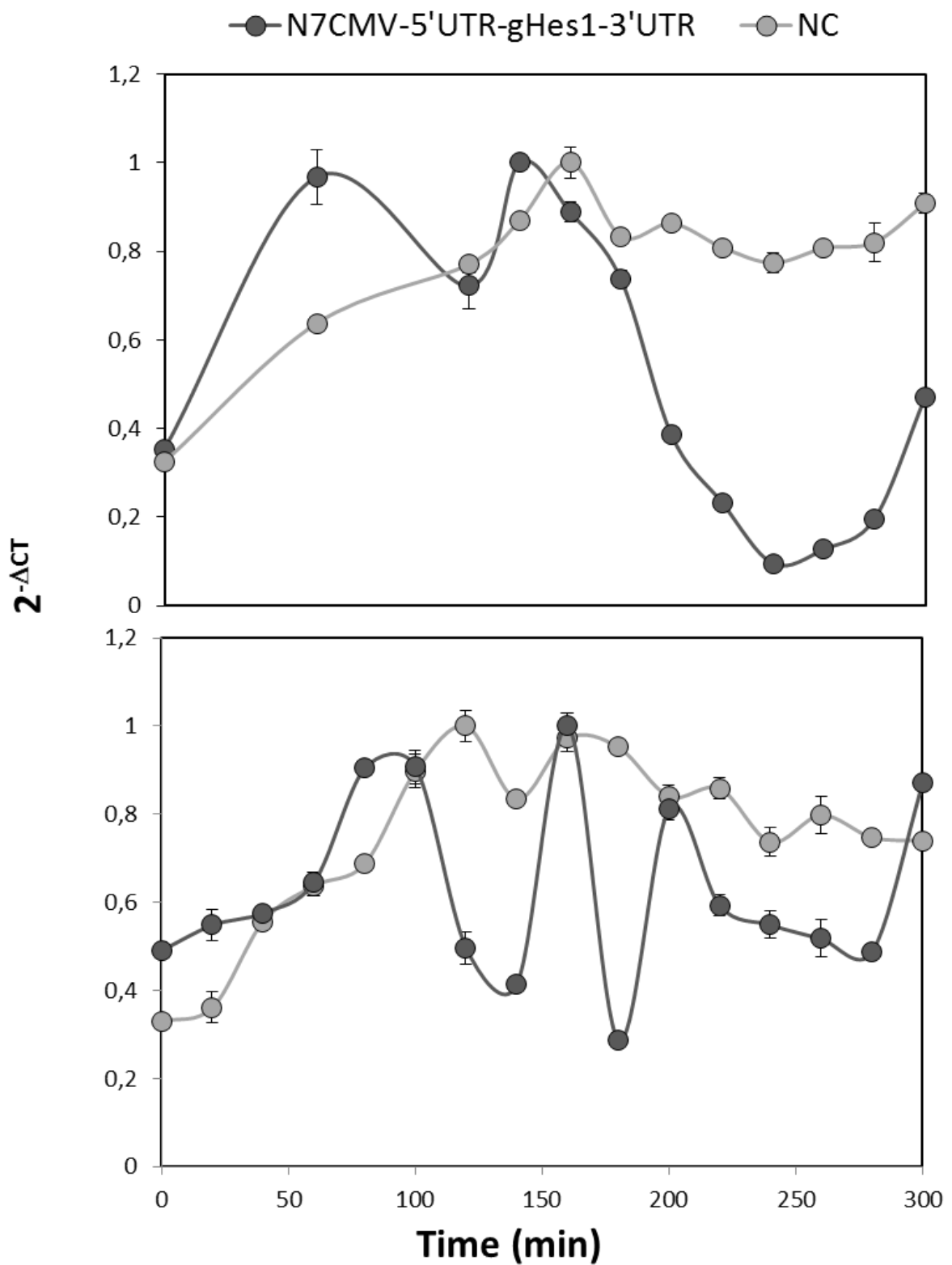
Figure 5.5 – Two replicates of the switch on experiment of *Hes1* oscillator. In light gray the negative control that is composed by N7CMV promoter expressing for the destabilized protein $Ub^{v76}eGFP$ that isn't able to repress its own promoter (Fig. 5.4b). In dark gray the dynamical behavior of the synthetic *Hes1* oscillator.

5.4 – Stable integration of *Hes1* oscillator in CHO cells

In order to reduce the experimental variability and obtain more clear results I produced 17 CHO-k1 monoclonal cell populations carrying stable integrations of N7CMV-5'UTR-gHes1-3'UTR construct (CHO-Syn-*Hes1*-Oscillator, CHO-SHO).
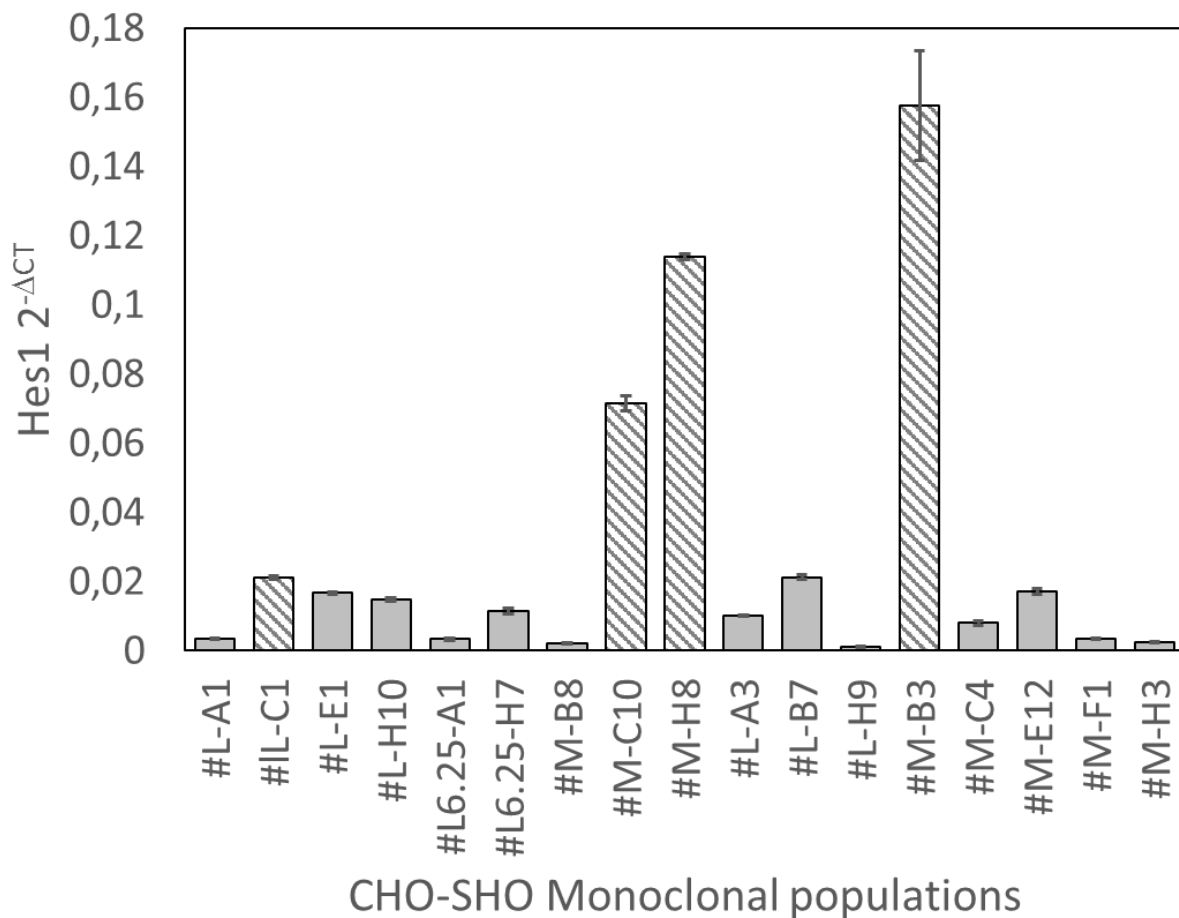
Figure 5.6 – Screening of the CHO-SHO monoclonal populations by qRT-PCR. X axes: monoclonal populations; Y axes: *Hes1* gene expression. The gray columns are the monoclonal cell population that express low level of *Hes1*. White columns with gray diagonals are the monoclonal cell populations that I tested to their ability to generate oscillations.

I then selected 4 clones which expressed *Hes1* at sufficient levels according to real-time qPCR (Figure 5.6). Then, I tested the CHO-SHO cells to their ability to generate oscillatory expression of the reconstituted *Hes1* gene. As for the transient transfection experiments, I synchronized the cell population by starvation and after 24 hours I activated the transcription
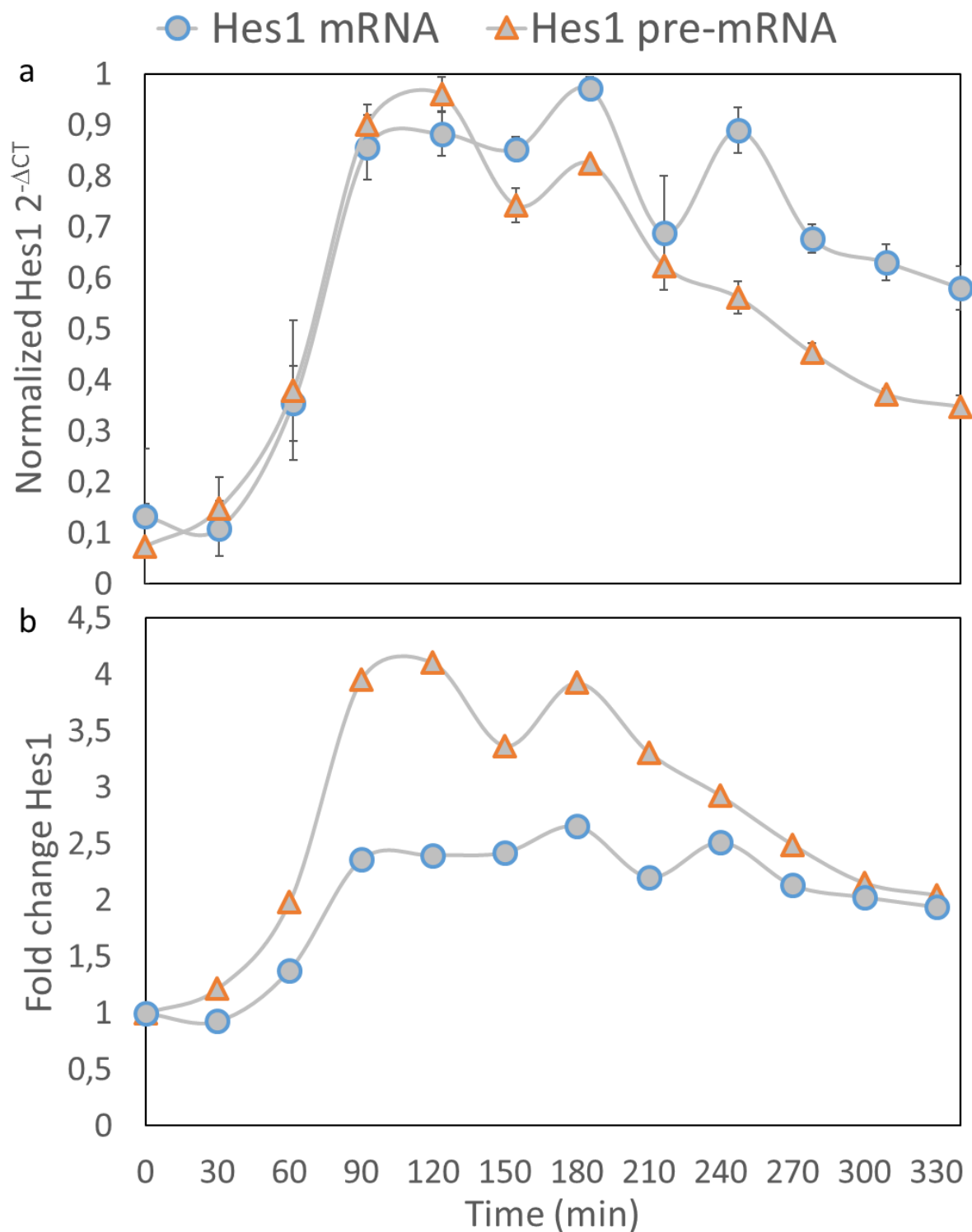
Figure 5.7 – Dynamical gene expression of the reconstituted *Hes1* Synthetic Oscillator in CHO K1 cells (CHO-SHO). X axes: time in minutes; Y axes: (a) Normalized values of the $2^{-\Delta CT}$ (b) Fold change of *Hes1* expression; The blue circles are the mature mRNA values; The orange triangles are the values for the pre-mRNA

by serum shock. Finally, I measured by RT-PCR the expression levels of *Hes1* pre-mRNA and

mature mRNA up to 330 minutes.

Only for one clone (clone #M-H8) I could observe a repression of the *Hes1* expression, as shown in Figure 5.7. Serum shock treatment leads to a strong transcriptional activation of both *Hes1* pre-mRNA and mRNA.

Moreover, the pre-mRNA is expressed before the mRNA suggesting the presence of a transcriptional delay of about 30 min (in line with the literature).

However, I could not detect multiple oscillations. This behavior could be explained either by a weak auto-inhibition in this specific clone, or a quick desynchronization of cell population. Therefore, to further characterize this system I need to implement a single cell approach based on a fluorescent reporter and time lapse microscopy.

5.5 – Toward single cell analysis: the fluorescent reporters

Since my focus is to generate a useful platform to study *Hes1* oscillations in single cells, I developed two strategies to visualize by time lapse microscopy the gene expression dynamics of *Hes1*. The first one is based on a monoclonal cell line with a double stable genome integration of N7CMV-5'UTR-gHes1-3'UTR oscillator and of the N7CMV-Ub^{v76}eGFP-3'UTR reporter construct (Fig. 5.7)
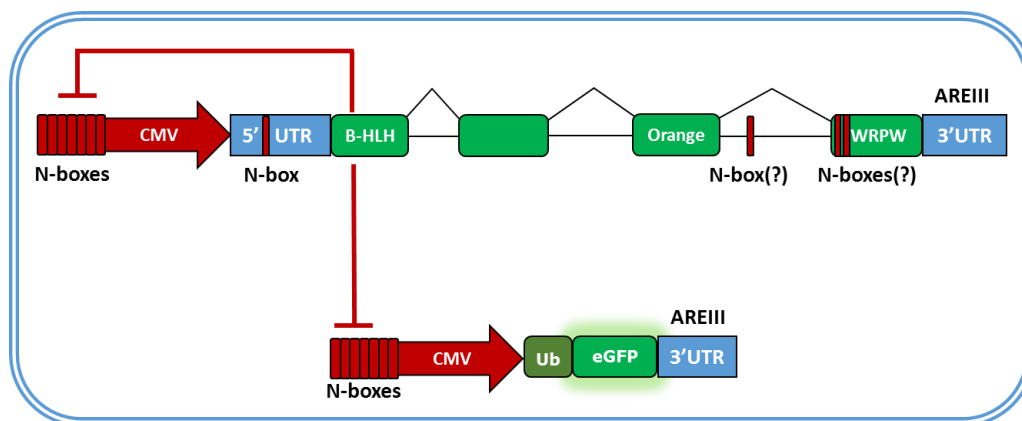
Figure 5.8 – Cartoon of the first strategy to visualize the *Hes1* expression in single cell (CHO-SHO 2.1). The N7CMV-5'UTR-gHes1-3'UTR repress itself and N7CMV-Ub^{v76}eGFP-3'UTR reporter by binding N7CMV promoters. The High destabilization of reporter protein given by the Ubiquitin moiety (Ub) and of mRNA given by 3'UTR allow the reporter to follow the *Hes1* expression

In particular, in the CHO-SHO cells described in section 5.4, I integrated the N7CMV-Ub^{v76}eGFP-3'UTR reporter (CHO-SHO 2.1). In this reporter construct, the expression of the destabilized fluorescent protein UbV76eGFP is driven by N7CMV promoter. Therefore, when HES1 is expressed, it binds the N7CMV promoters repressing itself and reporter expression that reflects *Hes1* oscillations.

In particular, in order to test the fluorescent reporter for its ability to follow *Hes1* oscillations, I used as cellular model a mouse myoblast cell line (C2C12), in which *Hes1* oscillations naturally happen after serum shock. The construct N7CMV-Ub^{v76}eGFP-3'UTR was transiently transfected in C2C12; after 8 hours I performed a starvation protocol followed by serum stimulation treatment.
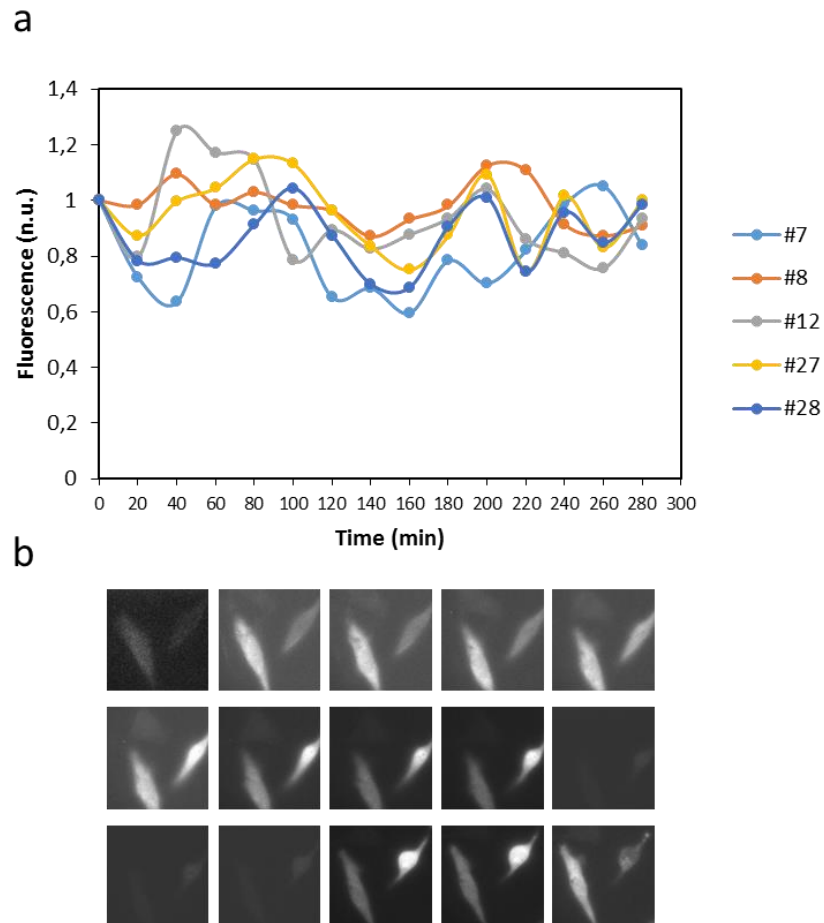
Figure 5.9 – Validation of N7CMV-Ub^{v76}eGFP-3'UTR reporter in C2C12 cells. **(a)** Plot of the segmented cells fluorescence; X axes: time in minutes, Y axes normalized fluorescent units. Each line is the expression dynamics Ub^{v76}eGFP for a single cell. **(b)** Image series of cells taken every 20 minutes with 60X magnification.

Then, I visualized the dynamics of N7CMV-Ub^{v76}eGFP-3'UTR reporter by time lapse fluorescent microscopy. By using a single cell automated segmentation algorithm implemented in Matlab environment, I quantified in single cell the changes in the fluorescence level in time. Therefore, from the data reported in figure 5.7 I can conclude that the reporter gene under investigation is able to follow the fast oscillations of endogenous *Hes1*.

The second strategy is based on a monoclonal cell line stably integrated with the N7CMV-5'UTR-gHes1-eGFP-3'UTR construct (CHO-SHO 2.2) represented in figure 5.9.
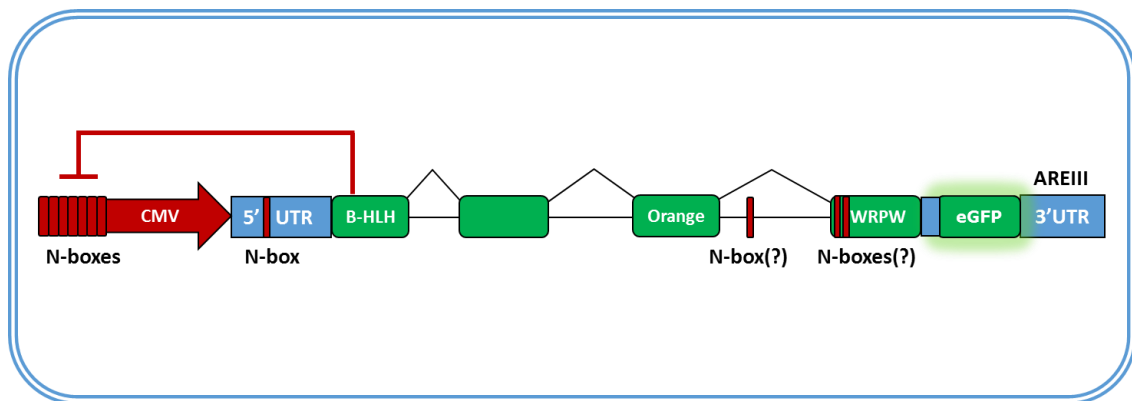
Figure 5.10 - Cartoon of the second strategy to visualize the *Hes1* expression in single cell (CHO-SHO 2.2). N7CMV-5'UTR-gHes1-eGFP-3'UTR is stable integrated in CHO K1 cells genome. The gHES1-eGFP fusion protein repress its own expression by binding N7CMV promoter and at the same time emits fluorescence

The CDS of the eGFP (enhanced Green Fluorescent Protein) was cloned between the *Hes1* genomic region and the *Hes1* 3'UTR, under the control of the synthetic promoter N7CMV. Ideally the fusion protein should work both as destabilized reporter and as repressor (5.8).

Therefore, in order to evaluate the destabilization degree of the fusion protein and of its mRNA

I cloned the gHes1-eGFP under the constitutive CMV promoter and I transfected this construct in CHO k1 cells.

Since, the expression level of a gene product at the steady state is function of its stability, I performed measurements 24 hours after transfection. Specifically, I measured gHes1-eGFP expression, both at mRNA (RT-PCR) and protein (FACS) levels. Finally, I compared the results with eGFP (stable reporter) and Ub^{v76}eGFP (destabilized reporter) used as controls.
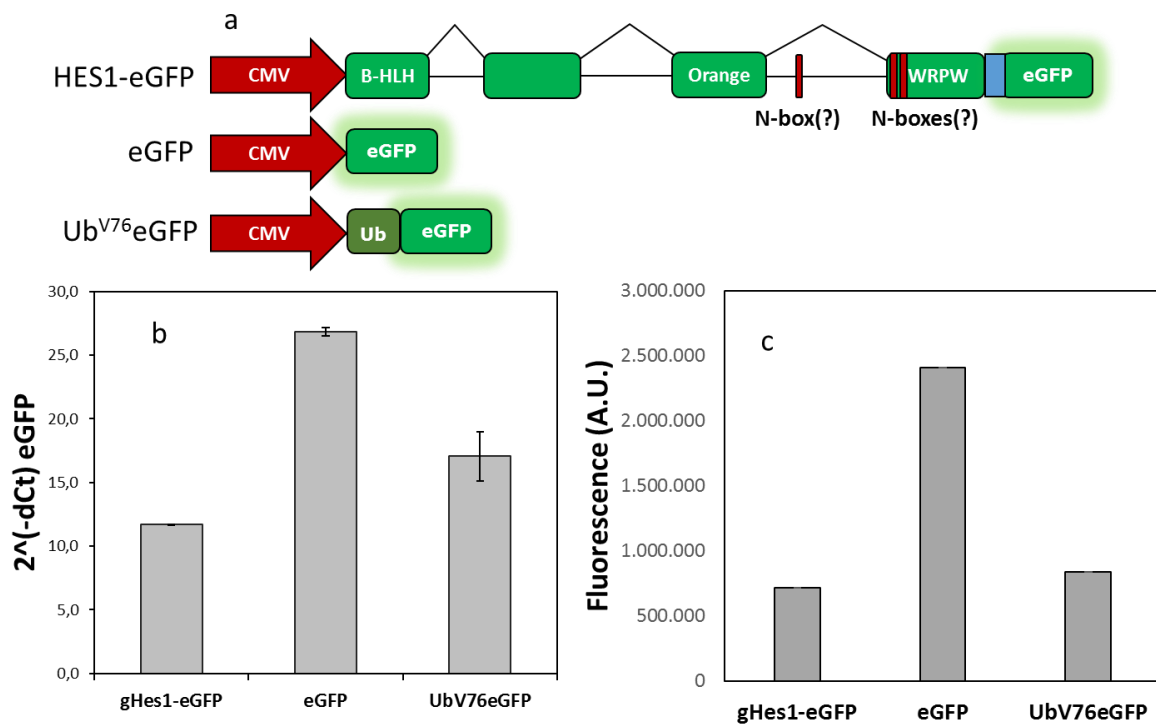
Figure 5.11 – Fusion protein stability validation. **(a)** Schematic representation of the construct used in the experiment. HES1-eGFP: fusion protein; eGFP stable fluorescent reporter; Ub^{V76}eGFP: unstable fluorescent reporter. **(b)** Steady state measurements of reporter mRNA (RT-PCR). **(c)** steady state measurements of the reporter protein (FACS).

As shown in Figure 5.10, at steady state the fusion protein HES1-eGFP is expressed at the lowest expression at both mRNA and protein levels. Therefore, I can conclude that gHes1-eGFP is a high destabilized reporter suitable to follow the quick changes in *Hes1* expression.

I also checked whether HES1 cloned in fusion with eGFP is still able to works as a repressor. To address this point, I cotransfected the CMV-gHes1-eGFP construct described before with the pHes1-Ub^{V76}Luc-3'UTR. This is a gene reporter for the natural promoter of *Hes1* (pHes1) that drives the expression of a destabilized luciferase.

I then performed a dose response curve keeping constant the amount of the promoter and increasing the amount of the gHes1-eGFP. Finally, I measured by RT-PCR the repression level of *Hes1*-eGFP and I compared it with the repression level of gHes1 (positive control) and of eGFP (negative control).

This experiment (Fig. 5.11), proves that even if HES1-eGFP shows a lower repression than HES1, nevertheless the two dose response curves (gHes1-eGFP and gHes1), when

compared to the eGFP (negative control), have a similar shape indicating strong repression of pHes1 by very low amount of HES1 protein.
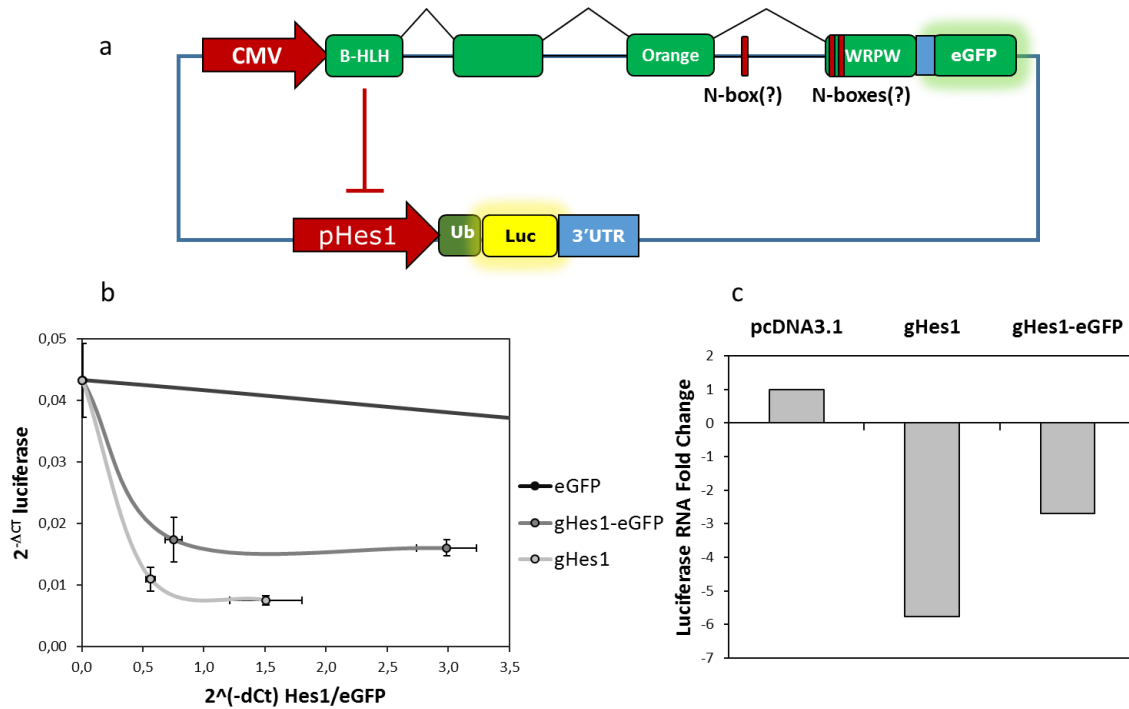
Figure 5.12 – Fusion protein validation for its ability to works as repressor. (a) Schematic representation of the experimental design: transfected gene network used to carry out the dose response curve of *Hes1* promoter, the network is composed by two plasmids, one expressing for the HES1-eGFP fusion protein and second plasmid expressing for a destabilized luciferase under the control of *Hes1* promoter region (pHes1). **(b)** plot of the dose response curve: In dark the data for the eGFP (negative control), In light gray the data for HES1 (positive control), in dark gray the data for the fusion protein HES1-eGFP. **(c)** Fold change of the repression values.

Therefore, I can conclude that the two fluorescent reporters, which I characterized, represent a very good tools to follow the *Hes1* oscillations in single cells.

Chapter 6 – Conclusions

A growing number of studies are revealing that cells can send and receive information by controlling the temporal behavior of a molecular species, such as a transcription factors (TFs). A typical example is represented by genetic oscillators, that transmit a great number of information in their amplitude and frequency[48].

In the last years, much efforts have been focused on the construction and analysis, of the synthetic genetic oscillator in order to better understand the relation between the structure and function of this genetic circuits. For example, by building a simple one gene negative-feedback synthetic clock, it has been demonstrated that intron length increases the oscillatory period of gene expression in mammalian cell[8]. Therefore, it can be hypothesized that this is one of the possible mechanisms that the evolution has selected over millions of years to fine tune the period of genetic oscillator. Other examples are provided by the construction of more complex synthetic gene networks. For example, oscillators in which the negative feedback is provided by antisense or small interfering RNAs have been shown to give rise to (unstable) oscillations in mammalian cells[3,11]. Generally speaking, it can be speculated that these particular kinds of non-coding RNAs can work as the "gears" of a complex clock.

In nature, several genetic clocks have been identified and were classified on the basis of the duration of their period. Oscillators with period longer than 24 hours are usually named circadian oscillators whereas those with period shorter than 24 hours are classified as ultradian oscillators. Of this last kind, a classical example is *Hes1* that is expressed with a period long about 2 hours in mice and with a period of about 5 hours in humans. The *Hes1* oscillations have been observed in several cellular types and developmental processes. For example, it has been shown that *Hes1* oscillations are required by the embryonic stem cells (ES) and by neuronal progenitor cells to maintain an undifferentiating sate. For this particular kind of dynamical behavior, several roles have been hypothesized, such as the maintenance of the correct timing of differentiation and the heterogeneous response of cells under the same environmental cues.

The mechanism underlying these oscillations in *Hes1* has been largely characterized in the literature. It is based on a delayed negative feedback loop, in which after a certain delay

given by the splicing process, the HES1 protein repress its own transcription by binding its own promoter. Although this mechanism has been well studied, mathematical and experimental evidences have suggested that a simple delayed negative feedback cannot explain the *Hes1* behavior in terms of robustness and percentage of oscillating cells[32].

For these reasons, in this work I focused my attention on the understanding the deeper mechanisms that underlie the dynamical behavior of *Hes1* and conversely its function.

Therefore, I first quantitatively characterized by an integrated computational and experimental approach the cis-regulatory elements of *Hes1* gene. Specifically, I focused my research on two aspects that nobody has investigated so far: the non-linearity of the negative feedback and the identification of the sequence responsible of rapid mRNA degradation. These two aspects are very important for *Hes1* oscillations, because the first one mediates the strong repression of the promoter and the second one avoids the accumulation of the mRNA inside the cell, permitting another transcriptional cycle.

Therefore, I started to quantitatively characterize the *Hes1* promoter region (pHes1) by a dose response curve, in this way I found that it can be well described by a high cooperativity Hill's function. In fact, by the numerical fitting of this function with experimental data I obtained that pHes1 is characterized by a high non-linearity (Hill's coefficient is equal to 7). This finding fits very well with the bifurcation analysis of a dynamical model of the *Hes1* clock in which I obtained oscillations only for Hill's coefficient greater than 2.

Moreover, in order to find the signal sequence responsible of the rapid *Hes1* mRNA degradation, I focused my attention on its 3'UTR. Indeed, it has been assumed that, as it happen for other mRNAs, the *Hes1* transcript instability could be regulated by the 3' untranslated region[24]. Therefore, by quantitative modeling and experimental data I found that *Hes1* 3'UTR shortens the mRNA half-life of a generic transcript to few seconds. In conclusion, for the first time I demonstrated that the 3'UTR of *Hes1* is the signal sequence responsible of the rapid *Hes1* mRNA degradation.

Following quantitative characterization of pHEs1 and the *Hes1* 3'UTR, I then moved to modular construction of a *Hes1* synthetic oscillator. Usually, genetic circuits are studied by genetic and biochemical perturbations, however the modularity of genes and proteins enables a complementary approach based on the construction and analysis of synthetic genetic circuits

inspired on their natural counterparts[49]. Since the role of each of the parts of *Hes1* oscillator is well characterized, I decided to reconstitute the *Hes1* oscillator in CHO-K1 cells. In particular, in order to understand if a delayed auto-inhibition is sufficient to give rise periodic *Hes1* expression, I produced a set of networks composed by both *Hes1* naturals parts and their synthetic analogs.

Therefore, first of all I produced and validated by a dose response curve a synthetic *Hes1* promoter analog, named N7CMV. Then, I cloned it upstream the *Hes1* genomic region (N7CMV-5'UTR-gHes1-3'UTR) and I analyzed this network in CHO-k1 cells. I tested this construct either via transient transfection or via stable genome integration (CHO-SHO cells).

The results that I obtained via transient transfection suggest that, in contrast to a negative control that rich a steady state in its gene expression, N7CMV-5'UTR-gHes1-3'UTR generates pulses and dynamic fluctuations of *Hes1* expression. However, I obtained a high variability of the experimental results that prevent me to better characterize this circuit. This experimental variability was overthrown in CHO-SHO cells, that nevertheless showing a very slow auto-inhibition.

Since I measured the gene expression across a whole cell population, in order to obtain more clear results, I decided to analyze my circuit at single cell level.

Indeed, individual cells differ widely in their dynamical responses also when they are synchronized. As a result, the average dynamical behavior of a population often represents a distorted version of individual behavior that can lead to misinterpretations. The development of fluorescent sensors that allow time-lapse imaging in living cells has improved our ability to quantify the dynamics of biological responses in single cells[48]. Thus, I developed and validated two fluorescent reporters of *Hes1* expression, one based on a destabilized Green fluorescent protein (Ub^{V76}GFP) and the second one based on the HES1-eGFP fusion protein. Specifically, I validated the N7CMV-Ub^{V76}GFP-3'UTR fluorescent construct, dynamically characterized in Chapter 3, for its ability to follow *Hes1* expression in C2C12, a cell line in which oscillations naturally happen. By time lapse fluorescent microscopy I found that this construct well recap in real time the *Hes1* oscillations. As I mentioned before, I also produced also a HES1-eGFP fusion protein that in addition to work as a fluorescent reporter, directly participates in the negative feedback. Therefore, I tested this reporter for its destabilization degree and for its

ability repress the *Hes1* promoter. I found that this fusion protein well works both as destabilized fluorescent reporter and as repressor of *Hes1* promoter.

I can conclude that these two reporter systems will allow me to study in single cell *Hes1* oscillations.

The next goals will be to characterize at single cell levels all of the genes networks presented in Chapter 4 in order to more deeply understand the how *Hes1* clock works. Specifically, I am interested in the circuit carrying the tetracycline inducible *Hes1* synthetic promoter, because I can switch off the circuit at will and by using microfluidic platform I can easily synchronize and control the *Hes1* expression dynamics.

Chapter 7 – Materials and method

7.1 - Cell culture

Chinese Hamster Ovary (CHO) cells were maintained at 37 °C in a 5% CO2-humidified incubator, and cultured in α-MEM (Sigma) supplemented with 10% heat-inactivated fetal bovine serum (FBS) (Invitrogen), 1% L-glutammine and 1% antibiotic/antimycotic solution (GIBCO BRL). C2C12 cells (ATCC® CRL-1772™) were purchased from American Type Culture Collection. Cells were grown with 4.5 g/l glucose-DMEM (Dulbecco's modified Eagle's medium; Gibco) supplemented with 100 units/ml penicillin/ 100 µg/ml streptomycin/1 mM glutamine (Sigma) and 10% foetal bovine serum (FBS) (Gibco) at 37 °C in 5% CO2. Cells were kept at low confluence. We observed consistent results only when using early passage cells (e.g., P2–P7).

7.2 - transfection reagents

Expression plasmids were transiently transfected using the TransIT-LT1 reagent (Mirus) according to the manufacturer. Where it is needed the total amount of DNA was equalized using the pcDNA3.1 empty vectors.

7.3 - Stable clones

Cells were transfected following TransIT-LT1 reagent (Mirus) according to the manufacturer protocol. Cells were maintained in antibiotics selection for 15 days. Then cells were sorted randomly or where it is possible for fluorescence intensity using a BD FACS Aria Cell Sorting System (Becton Dickinson). They were automatically plated in 96-well plate and maintained in antibiotics selection. Thus they were split in 6-well plate, then they were harvested to be analyzed by Real Time PCR. In cell lines were a fluorescent reporter was absent the screening were carried out by RT-PCR

7.4 - SS treatments

CHO cells were counted, and 300000 cells were plated in 30-mm dishes or 150000 in 6 wells plate and were grown in regular medium. After 24 h, were transfected and after 6 hours cells were washed twice with PBS (Phosphate Buffered Saline) [4.5 g/l glucose-DMEM (Gibco) supplemented with 100 units/ml penicillin/100 μg/ml streptomycin/ 1 mM glutamine (Sigma) and 0.2% FBS (Gibco)] and incubated for 24 h in starvation medium. Then, at various time points starvation medium was replaced with 10% FBS-containing growth medium, finally cells were collectedby using RLT buffer (QUIAGEN).

7.5 - mRNA expression analysis

Total RNA extraction was done using Rneasy kit (Quiagen) according to the manufacturer's instructions. Total RNA was then reverse-transcribed into cDNA using QuantiTect Reverse Transcription Kit (Quiagen) with random hexamers oligo. The cDNA was diluited 1:2 and subjected to quantitative real time PCR analysis by using: Light Cycler (Applied Biosystem) with SYBR Green PCR Master MIX Kit (Applied Biosystem) and with gene specific pair of primers, listed in the Table 7.1.

Table 7.1 Real time primers.

Gene	Forward primer	Reverse primer
Hes1 exon/exon junction	GGCCTCTGAGCACAGAAAG	TGCCGGGAGCTATCTTTC
Hes1 intron	CTCCGGAAATGGAGGGAGA	GTTGGACCGGTGCTAAACC
Gapdh	ACCCAGAAGACTGTGGATGG	GGATGCAGGGATGATGTTCT
eGFP	ACGACGGCAACTACAAGACC	GTCCTCCTTGAAGTCATGC
Luciferase	CAAGTGCGCTGCTGGTGCC	TTGGCAACCGCTTCCCCGAC
TTa	ACAGCGCATTAGAGCTG	ACCTAGCTTCTGGGCGAGTT

7.6 - Fluorescence Time-Lapse Microscopy

Image acquisition was performed using a Nikon Eclipse TI-E inverted epifluorescence microscope with a digital camera (iXon897, Andor), an incubation chamber (H201- OP R2, Okolab), a 40× objective (PlanFluor DLL 40× Ph2, Nikon), a YELLOW GFP BP HYQ filter (excitation 490–510 nm, emission 520–550 nm, Nikon). The exposure time for experiments in chamber slides was set to 30 ms for the phase-contrast images (with the transmitted-light lamp voltage set to 3 V), 100 ms for observation of $Ub^{V76}eGFP$. Images were acquired every 15 min The temperature was held constant at 37 °C, and the CO2 concentration was set to 5% of the total air volume injected into the incubation chamber. Experiments were performed and images were extracted using the NIS Elements AR software package, version 3.22.14, and the Perfect Focus System (Nikon Instruments) to maintain the focal plane throughout the experiment.

7.7 - FACS analysis

For the phenotypic analysis 18×10^4 or 25×10^4 cells were plated and allowed to grow for 24 after transfection. Cells were then harvested, washed and resuspended in 1 ml of PBS solution for cytofluorimetric analysis. Cells were analyzed with a BD accuri (Becton Dickinson) by using the FITC bandpass Filter (488 nm excitation, 525 emission) for $Ub^{V76}eGFP$. The distribution of 20000 events was recorded and used to calculate the mean fuorescence of each samples.

Bibliography

1.   Velia Siciliano, D. di B. E. A microRNA based genetic clock. (2011).

2.   Oudenaarden, S. M. and A. van. Synthetic biology: Understanding biological design from synthetic circuits. *Nat. Rev. Genet.* **10,** 859–871 (2009).

3.   Tigges, M., Marquez-Lago, T. T., Stelling, J. & Fussenegger, M. A tunable synthetic mammalian oscillator. *Nature* **457,** 309–312 (2009).

4.   Purcell, O., Savery, N. J., Grierson, C. S. & di Bernardo, M. A comparative analysis of synthetic genetic oscillators. *J. R. Soc. Interface* **7,** 1503–1524 (2010).

5.   Cheong, R. & Levchenko, A. Oscillatory signaling processes: The how, the why and the where. *Curr. Opin. Genet. Dev.* **20,** 665–669 (2010).

6.   Goodwin, B. C. Oscillatory behavior in enzymatic control processes. *Adv. Enzyme Regul.* **3,** 425–428 (1965).

7.   Stricker, J. *et al.* A fast , robust and tunable synthetic gene oscillator. **456,** (2008).

8.   Swinburne, I. A., Miguez, D. G., Landgraf, D. & Silver, P. A. Intron length increases oscillatory periods of gene expression in animal cells. 2342–2346 (2008). doi:10.1101/gad.1696108.al.

9.   Elowitz, M. B. & Leibler, S. A synthetic oscillatory network of transcriptional regulators. *Nature* **403,** 335–338 (1999).

10.   Müller, S. *et al.* Mathematical Biology A generalized model of the repressilator. 905–937 (2006). doi:10.1007/s00285-006-0035-9

11.   Tigges, M., Dénervaud, N., Greber, D., Stelling, J. & Fussenegger, M. A synthetic low-frequency mammalian oscillator. *Nucleic Acids Res.* **38,** 2702–2711 (2010).

12.   Smolen, P., Baxter, D. A., Byrne, J. H., Baxter, D. A. & Byrne, J. H. Frequency selectivity, multistability, and oscillations emerge from models of genetic regulatory systems. *Cell Physiol.* **274,** 531–542 (1998).

13.   Bratsun, D., Volfson, D., Tsimring, L. S. & Hasty, J. Delay-induced stochastic oscillations in gene regulation. *PNAS* **102,** 14593–14598 (2005).

14.   Venter, J. C. *et al.* The Sequence of the Human Genome. *Science (80-.).* **291,** 1305–1348 (2001).

15.   Ikeda, T., Matsuoka, T. & Satou, Y. A time delay gene circuit is required for palp formation in the ascidian embryo. *Development* **140,** 4703–8 (2013).

16.   Takashima, Y., Ohtsuka, T., González, A., Miyachi, H. & Kageyama, R. Intronic delay is essential for oscillatory expression in the segmentation clock. *Proc. Natl. Acad. Sci. U. S. A.* **108,** 3300–3305 (2011).

17. Mather, W., Bennett, M. R., Hasty, J. & Tsimring, L. S. Delay-Induced Degrade-and-Fire Oscillations in Small Genetic Circuits. *Phys. Rev. Lett.* **102,** 068105 (2009).

18. Dequeant, M.-L. *et al.* A Complex Oscillating Network of Signaling Genes Underlies the Mouse Segmentation Clock. *Science (80-.).* **314,** 1595–1598 (2006).

19. Taeko Kobayashi, R. K. in *bHLH Transcription Factors in Development and Disease* 263–283 (2014).

20. Kageyama, R., Ohtsuka, T. & Kobayashi, T. The Hes gene family: repressors and oscillators that orchestrate embryogenesis. *Development* **134,** 1243–1251 (2007).

21. Iso, T., Kedes, L. & Hamamori, Y. HES and HERP families: Multiple effectors of the notch signaling pathway. *J. Cell. Physiol.* **194,** 237–255 (2003).

22. Ishibashil, M. & Moriyoshi, K. Persistent expression of helix -loop -helix factor HES-1 prevents mammalian neural differentiation in the central. **13,** 1799–1805 (1994).

23. Shawber, C. *et al.* Notch signaling inhibits muscle cell differentiation through a CBF1-independent pathway. *Development* **122,** 3765–3773 (1996).

24. Hirata, H. Oscillatory Expression of the bHLH Factor *Hes1* Regulated by a Negative Feedback Loop. *Science (80-.).* **298,** 840–843 (2002).

25. Kageyama, R., Ohtsuka, T. & Kobayashi, T. Roles of Hes genes in neural development. *Dev Growth Differ* **50 Suppl 1,** S97–103 (2008).

26. Kageyama, R., Ohtsuka, T., Shimojo, H. & Imayoshi, I. Dynamic Notch signaling in neural progenitor cells and a revised view of lateral inhibition. **11,** 1247–1251 (2008).

27. Sasai, Y., Kageyama, R., Tagawa, Y., Shigemoto, R. & Nakanishi, S. Two mammalian helix-loop-helix factors structurally related to Drosophila hairy and Enhancer of split. *Genes Dev.* **6,** 2620–2634 (1992).

28. Fisher, A. L. & Ohsako, S. The WRPW Motif of the Hairy-Related Basic Helix-Loop-Helix Repressor Proteins Acts as a 4-Amino-Acid Transcription Repression and Protein-Protein Interaction Domain. **16,** 2670–2677 (1996).

29. Paroush Z , Finley Jr RL , Kidd T , Wainwright SM , Ingham PW , Brent R, I.-H. D. Groucho is required for Drosophila neurogenesis , segmentation , and sex determination and interacts … Groucho Is Required for Drosophila Neurogenesis , Segmentation , and Sex Determination and Interacts Directly with Hairy-Related bHLH Proteins. *Cell* **79,** 805 – 815 (1995).

30. Iso, T. *et al.* HERP , a Novel Heterodimer Partner of HES / E (spl) in Notch Signaling. **21,** 6080–6089 (2001).

31. Yoshiura, S. *et al.* Ultradian oscillations of Stat, Smad, and *Hes1* expression in response to serum. *Proc. Natl. Acad. Sci. U. S. A.* **104,** 11292–11297 (2007).

32. Masamizu, Y. *et al.* Real-time imaging of the somite segmentation clock: revelation of

unstable oscillators in the individual presomitic mesoderm cells. *Proc Natl Acad Sci U S A* **103,** 1313–1318 (2006).

33.   Kang, S. A., Seol, J. H. & Kim, J. The conserved WRPW motif of Hes6 mediates proteasomal degradation. *Biochem. Biophys. Res. Commun.* **332,** 33–6 (2005).

34.   Ohtsuka, T., Ishibashi, M., Gradwohl, G., Nakanishi, S. & Kageyama, R. *Hes1* and Hes5 as Notch effectors in mammalian neuronal differentiation. **18,** 2196–2207 (1999).

35.   Nakayama, K. & Satoh, T. FGF induces oscillations of *Hes1* expression and Ras / ERK activation. **18,** 332–334

36.   Ying, Q., Nichols, J., Chambers, I. & Smith, A. BMP Induction of Id Proteins Suppresses Differentiation and Sustains Embryonic Stem Cell Self-Renewal in Collaboration with STAT3. **115,** 281–292 (2003).

37.   Kobayashi, T. *et al.* The cyclic gene *Hes1* contributes to diverse differentiation responses of embryonic stem cells. 1870–1875 (2009). doi:10.1101/gad.1823109.1870

38.   Kobayashi, T. & Kageyama, R. *Hes1* regulates embryonic stem cell differentiation by suppressing Notch signaling. 689–698 (2010). doi:10.1111/j.1365-2443.2010.01413.x

39.   Artavanis-tsakonas, S., Rand, M. D. & Lake, R. J. Notch Signaling : Cell Fate Control and Signal Integration in Development. *Signal Transduct.* **284,** 770–776 (1999).

40.   Shimojo, H., Ohtsuka, T. & Kageyama, R. Oscillations in Notch Signaling Regulate Maintenance of Neural Progenitors. *Neuron* **58,** 52–64 (2008).

41.   Takebayashi, K. *et al.* Structure, chromosomal locus, and promoter analysis of the gene encoding the mouse helix-loop-helix factor HES-1: Negative autoregulation through the multiple N box elements. *J. Biol. Chem.* **269,** 5150–5156 (1994).

42.   Goldberg, D. E. *Genetic Algorithms in Search , Optimization , and Machine Learning*. (1989).

43.   Chen, C. A. & Xu, N. mRNA Decay Mediated by Two Distinct AU-Rich Elements from c-fos and Granulocyte-Macrophage Colony-Stimulating Factor Transcripts : Different Deadenylation Kinetics and Uncoupling from Translation. **15,** 5777–5788 (1995).

44.   Bonev, B., Stanley, P. & Papalopulu, N. MicroRNA-9 Modulates *Hes1* Ultradian Oscillations by Forming a Double-Negative Feedback Loop. *CELREP* **2,** 10–18 (2012).

45.   Harima, Y., Takashima, Y., Ueda, Y., Ohtsuka, T. & Kageyama, R. Accelerating the Tempo of the Segmentation Clock by Reducing the Number of Introns in the Hes7 Gene. *Cell Rep.* **3,** 1–7 (2013).

46.   Clontech protocol: Tet-On 3G Inducible Expression System. at <https://www.clontech.com/US/Products/Inducible_Systems/Tetracycline-Inducible_Expression/ibcGetAttachment.jsp?cItemId=39657&fileId=6471780>

47.   Loew, R. & Heinz, N. Improved Tet-responsive promoters with minimized background

expression. *BMC Biotechnol.* **10,** 81 (2010).

48.   Purvis, J. E. & Lahav, G. Encoding and Decoding Cellular Information through Signaling Dynamics. *Cell* **152,** 945–956 (2013).

49.   Sprinzak, D. & Elowitz, M. B. Reconstruction of genetic circuits. **438,** 443–448 (2005).